THE INFLUENCE OF TERRESTRIAL MATTER IN MARINE FOOD WEBS OF THE BEAUFORT SEA SHELF AND SLOPE

By

Lauren Bell

RECOMMENDED:

Dr. Bodil Bluhm

Dr. Matthew Wooller

Dr. Steve Okkonen

Dr. Katrin Iken
Advisory Committee Chair

Dr. Katrin Iken
Program Head, Marine Sciences and Limnology

APPROVED:

Joan Braddock
Dr. Joan Braddock
Interim Dean, School of Fisheries and Ocean Sciences

John C Eichelberger
Dr. John Eichelberger
Dean of the Graduate School

24 April 2015
Date

THE INFLUENCE OF TERRESTRIAL MATTER IN MARINE FOOD WEBS OF THE BEAUFORT SEA SHELF AND SLOPE

A

THESIS

Presented to the Faculty
of the University of Alaska Fairbanks

in Partial Fulfillment of the Requirements
for the Degree of

MASTER OF SCIENCE

By

Lauren Bell, B.S.

Fairbanks, Alaska

May 2015

Abstract

Terrestrial organic matter (OM_{terr}) can function as a food source for Arctic marine consumers, though the relative contribution of OM_{terr} to the structure and efficiency of marine food webs compared to marine production is unclear. Forecasted increases in OM_{terr} inputs to the Arctic Beaufort Sea necessitate a better understanding of the proportional contribution of this organic matter source to the trophic structure of marine communities. This study investigated the relative ecological importance of OM_{terr} across the Beaufort Sea shelf and slope by examining differences in community trophic structure concurrent with variation in terrestrial versus marine organic matter influence. Hydrogen stable isotope ratios (δD) of surface water, surface sediment particulate organic matter (sPOM), and selected benthic consumers were used as an exploratory assessment of freshwater and OM_{terr} distribution in the Beaufort Sea. δD values of surface water confirmed the widespread influence of Canada's Mackenzie River plume across the Beaufort Sea; however, δD values of terrestrial and marine production were not sufficiently distinguishable to differentiate organic matter sources in consumers. Carbon stable isotope ratios ($\delta^{13}C$ values) of pelagic particulate organic matter (pPOM) and marine consumers confirmed a significant decrease in OM_{terr} presence and utilization by consumers with increasing distance from the Mackenzie River outflow. Food web length, based on the nitrogen stable isotope ratios ($\delta^{15}N$ values) of marine consumers, was longer closer to the Mackenzie River outflow both in shelf and slope locations due to relatively higher $\delta^{15}N$ values of pelagic and benthic primary consumers. The absence of macrofaunal consumers at the lowest trophic levels of OM_{terr}-influenced food webs was interpreted to result from the prior metabolic turnover of OM_{terr} by the microbial loop, which was not sampled in this study. The inferred presence of strong microbial processing of OM_{terr} in the eastern regions of the Beaufort Sea resulted in a higher proportion of relative epifaunal biomass occupying higher trophic levels, suggesting that OM_{terr} as a basal food source can provide substantial energetic support for higher marine trophic levels. These findings challenge the current conception of low terrestrial matter contributions to the Arctic marine food web, and compel a more specific understanding of energy transfer through the OM_{terr}-associated microbial loop.

Table of Contents

Page

Signature Page i

Title Page iii

Abstract v

Table of Contents vii

List of Figures ix

List of Tables xi

List of Appendices xiii

Acknowledgements xv

Introduction 1

Methods 5

Study area 5

Sampling and at-sea processing 6

Lab processing and stable isotope analysis 11

Data analysis: δD values 12

Data analysis: $\delta^{13}C$ *and* $\delta^{15}N$ *values* 14

Results 19

Large-scale water mass structure 19

Spatial distribution and influence of terrestrial organic matter 23

Regional and depth variation in food web structure 30

Discussion 37

Freshwater and terrestrial matter distribution and utilization 37

Trophic structure by depth and terrestrial matter influence 42

Conclusion 47

References 49

Appendices 61

List of Figures

Page

Figure 1: Map of stations sampled in the Beaufort Sea 7

Figure 2. Regionally averaged vertical sections of water temperature, salinity, and δD values 20

Figure 3. δD values (‰) of water samples taken from the surface (**A**) and 10 m depth (**B**) in the 2013 sampling area 21

Figure 4. Trends in δD values of surface water, sediment particulate organic matter (sPOM), and selected benthic consumers by bottom depth in each region of the eastern Beaufort Sea 22

Figure 5. Biplot of $\delta^{13}C$ and $\delta^{15}N$ values for pPOM and sPOM compared alongside potential POM endmembers in the eastern Beaufort Sea 28

Figure 6. Carbon to nitrogen ratios, $\delta^{13}C$ and $\delta^{15}N$ values of pPOM and sPOM with station bottom depth, averaged by region 29

Figure 7. Mean (±SD) $\delta^{13}C$ values (‰) of possible food sources (pPOM and sPOM; shaded background) and consumer feeding guilds (white background), by region and depth group (shelf or slope) 31

Figure 8. Select benthic consumers' $\delta^{15}N$ values (‰) by bottom depth on log-scale, across all regions 32

Figure 9. Trophic positions of all consumers by shelf and slope regions 34

Figure 10. Relative biomass of consumers within each trophic level based on using a primary consumer baseline (see Fig. 9B), by shelf and slope regions 35

Figure A-1. Relative distribution of the number of taxa by trophic level for full taxon set 61

Figure A-2. Relative distribution of the number of taxa by trophic level, including only the subset of taxa chosen for relative biomass comparison 61

List of Tables

Page

Table 1. Station locations and types of isotope samples collected for this study 8

Table 2. Mean $\delta^{13}C$ and $\delta^{15}N$ values (‰) of pPOM, sPOM, and sampled taxa by region and depth group (shelf or slope)...24

List of Appendices

Page

Appendix A. Comparison of relative taxa distribution for biomass analysis 61

Appendix B. 2013 IACUC #134765-13 approval 62

Appendix C. 2014 IACUC #134765-14 approval 63

Acknowledgements

This large project would not have been possible without all of the generous support I received along the way. First of all, a very big thank you to the Bureau of Ocean Energy Management for providing the majority of funding for this project, and to Kate Wedemeyer, the BOEM Project Officer, for her organizational support. I also received generous support from the UAF Center for Global Change Student Research Grant with funds from the Cooperative Institute for Alaska Research, as well as from the Arctic Institute of North America Grant-in-Aid Program and the Robert and Kathleen Byrd Award. I am grateful to the UAF Graduate School for providing my last semester's worth of funding through the Graduate School Thesis Completion Grant.

I would like to thank the crew of the R/V Norseman II and the logistics superstars at Olgoonik/Fairweather who enabled the 40+ days of efficient and enjoyable sampling in the Beaufort Sea that provided the data for this project. The opportunity to collaborate with three other UAF labs while at sea and when back in Fairbanks allowed me to broaden my analysis to include taxa and oceanographic data that lay outside of my sampling expertise: many thanks to Russell Hopcroft and Caitlin Smoot for CTD data and zooplankton samples, Sarah Hardy and Julia Dissen for infauna samples, and Brenda Norcross's entire lab for sharing many samples of fish tissue (IACUC no. 134765). A big thank you to all the invertebrate taxonomists across the world who verified the more challenging-to-identify taxa in this analysis. Mette Kaufmann and Douglas Duncan were both invaluable lab technicians during my slog through a few thousand isotope samples – thank you both for your technique tips and your extra hands in the lab. And, it was truly the smiling faces and constant laughter from Tim Howe and Norma Haubenstock at the Alaska Stable Isotope Facility that made the many trips across campus to weigh animal tissue such a pleasure (even in -40°F temperatures).

I was so fortunate to have a diverse and supportive committee who were patient with me as I found my way through my sea of data and attempted to make sense of it all. Mat Wooller gave me the tools to speak "isotope-ese" with confidence, and always managed to renew my excitement over my project with his infectious enthusiasm for 'beautiful isotope data'. Steve Okkonen was an invaluable resource when it came to the oceanographic features of the Beaufort Sea, never seeming to tire over answering my most basic of questions. Thank you, Steve, for hanging in through the hours of isotope talk, and sticking with me over bad internet and phone connections along the way. It was a pleasure to have the opportunity to work alongside Bodil

Bluhm on several cruises, as she proved that passion for work can shine just as bright at 4 am and after a 16 hour shift – especially if there is a bizarre species on your tray that could be keyed out! Bodil has been such a mentor and friend in and out of the workplace, and I credit her for helping me to fall in love with Sitka, which has become my new home. Lastly, I am so incredibly grateful to Katrin Iken for having taken me on as a graduate student for a project and study area that were very new to me. Katrin has been an inspiration in her approach to research and teaching, and has become a very dear friend during the last two and a half years. I am honored to be able to call her my advisor, and if I can someday become half the scientist that she is, I think I will have done pretty all right. Thank you times infinity, Katrin, and cheers!

Finally - my family, my friends, Dane, and sweet Leo: you were my backbones during this adventure. My life is so much richer with all of you in it, and my heart many times larger. Thank you for all of your encouragement and love along the way.

Introduction

Coastal erosion and river discharge along the Arctic U.S.-Canada coastline result in the deposition of large amounts of terrestrially-derived organic matter (OM_{terr}) into the Beaufort Sea of the Arctic Ocean (Macdonald et al. 1998; Rachold et al. 2004; McClelland et al. 2012; Goñi et al. 2013; McClelland et al. 2014). Compared with marine production, OM_{terr} is refractory, nutrient-poor, and reputed to be difficult for marine primary consumers to assimilate directly (Cividanes et al. 2002; Dunton et al. 2012). The additional microbial decomposition that is needed to transform OM_{terr} into a useable food source for marine consumers (Tenore 1983; Parsons et al. 1988; Garneau et al. 2009) has historically been presumed to result in inefficient energy transfer from OM_{terr} to higher trophic levels of marine food webs (Schell 1983; Dunton et al. 1989; Pomeroy and Deibel 1986; Berglund et al. 2007). Marine environments with tight coupling between primary production and benthic consumers are often considered indicative of high energy transfer efficiency because of the short trophic pathway from baseline food source to consumers (Hobson et al. 1995; Dunton et al. 2005; Carmack and Wassmann 2006; Iken et al. 2010; Feder et al. 2011; Hansen et al. 2012). Following this reasoning, the longer food webs resulting from additional trophic steps involved in microbial metabolism of OM_{terr} could be symptomatic of a poor-quality food source and inefficient energy transfer (e.g., Rosenzweig 1971; Pomeroy and Wiebe 1988; Abrams and Roth 1994).

Nearshore lagoons and river deltas of the Beaufort Sea contain, contrary to previous assumptions, surprisingly productive biological communities where OM_{terr} functions as a primary food source (Dunton et al. 2012; Ortega-Retuerta et al. 2012; Casper et al. 2014). Modern food web theory proposes that food web length is not solely indicative of system productivity or efficiency, but is a result of many complex and interrelated system attributes, such as ecosystem size, resource availability, or vulnerability to disturbance (Post 2002a; Arim et al. 2007). Furthermore, terrestrially-associated microbial metabolism is becoming increasingly understood as both a highly efficient and quality-enhancing process, functioning as a trophic connection between OM_{terr} and marine consumers (Klein Breteler et al. 1999; Lefébure et al. 2013; Rontani et al. 2014). Thus, past presumptions of OM_{terr} as a poor food source for marine consumers based solely on food web length are likely incorrect.

The goal of this study was to examine the extent to which OM_{terr} influences the offshore Arctic marine food webs of the Beaufort Sea, from shelf to basin. In addition to the large vector that coastal erosion provides for OM_{terr} into the Alaskan Beaufort (Goñi et al. 2013), Canada's Mackenzie River in the eastern Beaufort Sea delivers more terrestrially-derived particulate organic carbon (POC) to the Arctic Ocean (1.8×10^{12} g POC yr^{-1}; Telang et al. 1991) than all other Arctic rivers combined (Rachold et al. 2004). Increasing presence and biological utilization of OM_{terr} with proximity to the Mackenzie Delta has been inferred from stable isotope values of food sources and biota on the Beaufort shelf westward of the river (Dunton et al. 1989; Saupe et al. 1989; Schell et al. 1998; Goñi et al. 2000; Naidu et al. 2000). Though this east-to-west, along-shelf gradient of OM_{terr} influence from the Mackenzie River affects trophic structure in the nearshore Beaufort Sea (Dunton et al. 2006, 2012), it is unknown to what extent it is reflected in the benthic marine food webs farther offshore on the shelf and on the slope into the Arctic basin. The potential of terrigenous carbon to influence food webs on the outer Beaufort shelf and slope is high: satellite images have captured the sediment plume exiting the Mackenzie River extending more than 400 km off-shelf (Macdonald et al. 1999) and high fluxes of terrestrially-derived carbon have been recorded in the water column over the 500-m isobath of the slope (Forest et al. 2007). In addition, sinking time and microbial processes associated with water depth affect the degree to which organic material undergoes bacterial degradation and remineralization (Macko and Estep 1984; Wassmann 1998; Robinson et al. 2012). Therefore, deep-sea benthic food webs can be primarily dependent on highly-recycled organic matter deposited on the abyssal floor (Iken et al. 2001, 2005). Hence, regardless of the initial origins of the organic matter supporting food webs along a depth gradient, increasing bottom depth is likely to indirectly impact trophic structure.

Tracking of organic matter provenance and energy flow in aquatic food webs is commonly accomplished using the well-vetted technique of stable isotope analysis (Michener and Lajtha 2007). Carbon derived from terrestrial plant production at high latitudes is isotopically lighter (Wooller et al. 2007) than carbon formed from marine primary production (Naidu et al. 1993, and references therein), so that the carbon stable isotope ratio ($\delta^{13}C$) of an organic matter sample can indicate the relative endmember source composition of that sample. While OM_{terr} often represents a complex mixture of sources, such as freshwater aquatic production, modern terrestrial plant production, and ancient eroded peat (Goñi et al. 2005), the $\delta^{13}C$ value of OM_{terr}

remains distinctly lower than marine production regardless of its specific composition. Nitrogen stable isotope ratios (δ^{15}N values) show a stepwise enrichment of the heavier isotope (^{15}N) between food source and consumer due to trophic fractionation (Vander Zanden and Rasmussen 2001; Post 2002b), allowing for the creation of food webs based on the δ^{15}N values of consumers relative to their baseline food source. In addition to measuring the δ^{13}C and δ^{15}N values of organic matter, oxygen and hydrogen stable isotope ratios (δ^{18}O and δD values) of surface waters can be used to trace the mixing of a freshwater source into the marine system, thereby providing an additional proxy of a potential pathway of OM_{terr} contained in this freshwater into the Arctic Ocean. δ^{18}O and δD values of precipitation vary predictably in relation to each other along the global meteoric water line (GMWL) (Craig 1961), imparting specific isotopic values to high latitude, river-derived freshwater. This enables the use of these isotopes to distinguish whether freshwater mixing into an Arctic marine system originated from a river or from surface sea ice-melt (Krouse and Mackay 1971; Cooper et al. 2005; Lansard et al. 2012). In my study, I used these isotopes to track freshwater from the Mackenzie River plume in the surface waters over the Beaufort Sea shelf and slope.

A recent surge in the use of δD values of organic matter to trace terrestrially-derived versus marine-derived production in aquatic systems (Doucett et al. 2007; Finlay et al. 2010; Soto et al. 2013) motivated the inclusion of organic matter δD ratios in this study to complement the classical δ^{13}C value analyses. Deuterium presents a potentially valuable tool for differentiating between terrestrial and marine organic matter sources, as deuterium isotope discrimination between water and organic matter during photosynthesis is much greater in phytoplankton than in terrestrial plants (Hondula et al. 2014; Yang et al. 2014). The isotopic separation between terrestrial and marine production δD values is in some cases far greater than in corresponding δ^{13}C values, allowing for higher resolution between the two endmembers (e.g., Doucett et al. 2007). However, to define the influence of terrestrial versus marine production on marine consumers and food web structure in the Beaufort Sea, the endmember values of these organic matter sources have to be directly measured, which so far has proven technically difficult in this region. Therefore, an exploratory δD assessment of organic matter and animal tissue was attempted in this study.

Food webs can track change in Arctic marine ecosystems because trophic structure is directly affected both by variation in the quality and quantity of primary production entering the base of the food web (Søreide et al. 2006; Bluhm and Gradinger 2008) as well as by water mass characteristics (Iken et al. 2010) that may be subject to change. The Arctic is projected to be strongly affected by climate change (ACIA 2004; Trenberth et al. 2007; Walsh 2008), and predicted changes on the Beaufort Sea shelf include a decrease in seasonal ice-cover (Frey et al. 2014) and an increase in coastal erosion and terrigenous carbon inputs (Lantuit et al. 2012; Holmes et al. 2013). Through food web connections, such changes have high potential to impact fish populations and mammal species critical to the numerous subsistence communities along Alaska and Canada's northern coasts (Ford and Smit 2004; Lowry et al. 2004; Crawford et al. 2012). Elucidating the relative importance of terrestrial- and marine-derived organic matter inputs to the marine food webs of the Beaufort shelf and slope will greatly enhance our ability to forecast some effects of climate change across the Arctic ecosystem.

The objectives of this study were, therefore, to 1) use carbon and hydrogen stable isotopes to identify the relative distribution and biological assimilation of terrestrially-derived organic matter in invertebrate and fish consumers across the Beaufort Sea shelf and slope, and 2) use carbon and nitrogen stable isotopes to analyze variations in the trophic organization of consumers among regions of the Beaufort shelf and slope.

Methods

Study area

The Beaufort Sea is a seasonally ice-covered and hydrodynamically complex Arctic system, with highest riverine inputs into the shallow shelf waters in the east (Macdonald et al. 1998; Carmack and Wassmann 2006), the strongest influence of productive Chukchi Sea waters to the west (Okkonen et al. 2009), and warmer, deeper basin water derived from the Atlantic Ocean occasionally upwelled along the steep slope (Tremblay et al. 2011). The Beaufort shelf is only 80-100 m deep at its abrupt shelf-break 80 to 120 km offshore, after which the slope can dive to 1000 m over a horizontal distance of only a few kilometers (Münchow and Carmack 1997; Kulikov et al. 1998; Pickart 2004). Over this bathymetric relief, the following interacting water masses layer vertically (Lansard et al. 2012): freshwater from rivers and sea ice-melt forms a thin surface lens (0-10 m) over the Pacific-derived polar mixed layer (Macdonald et al. 1989), which can be separated by a pycnocline at around 120 m water depth from the cold and highly nutrient-rich upper halocline layer (Shimada et al. 2005). At around 200 m, there is a transition to warmer and more saline Atlantic-derived water, which gradually transitions into the cold Canada Basin deep water below approximately 800 m depth (Lansard et al. 2012). Each water mass is distinct in temperature, salinity, nutrient concentration, and organic matter composition (Macdonald et al. 1989). Such differences have been linked to variation in food web structure in nearby systems, for example, on the shallow Beaufort Sea nearshore (Dunton et al. 1989, 2006, 2012), on the Chukchi Sea shelf (Iken et al. 2010), and in the deep Arctic Canada Basin (Iken et al. 2005). Upwelling events related to easterly winds advect nutrients and recycled marine production upwards to the consumers living on the Beaufort shelf (Pickart et al. 2013), while resuspension processes and aggregation mechanisms of biogenic matter can result in a large vertical flux of organic matter from the Beaufort shelf down the slope (Hwang et al. 2010; Forest et al. 2013).

In addition to this vertical structure, high freshwater outflow from Canada's Mackenzie River between May and September brings suspended inorganic sediment (127 Tg yr^{-1}) and OM$_{terr}$ (3.4 Tg total C yr^{-1}) into the oceanic water masses of the eastern Beaufort Sea (Macdonald et al. 1998). OM$_{terr}$ inputs from the Mackenzie River dwarf contributions of OM$_{terr}$ into the Beaufort from other vectors, such as coastal erosion (~0.5 Tg C yr^{-1}; Rachold et al. 2000; Ping et al. 2011) and the next three largest rivers in the Beaufort region: the Colville, Kuparuk, and Sagavanirktok rivers (~0.3 Tg C yr^{-1}; McClelland et al. 2014). As such, the Beaufort Sea is characterized by a distinct gradient of increasingly diluted freshwater and OM_{terr} with horizontal distance from the Mackenzie Delta and with increasing depth across the shelf and slope (Macdonald et al. 1995; Carmack and Macdonald 2002; Macdonald et al. 2002; Connelly et al. 2012; Brown et al. 2014).

Sampling and at-sea processing

Water, particulate organic matter (POM), invertebrate and fish samples were collected in 2012 and 2013 in the Beaufort Sea aboard the R/V *Norseman II*, under the Bureau of Ocean Energy Management (BOEM) Cooperative Agreement No. M12AC00011, "U.S.-Canada Transboundary Fish and Lower Trophic Communities", U.S. Department of the Interior, BOEM, Alaska Outer Continental Shelf Region, Anchorage, Alaska, as part of the BOEM Environmental Studies Program. The primary target regions were the central Beaufort Sea in 2012 and the eastern Beaufort Sea in 2013. From 21-30 September 2012, 19 stations along three shelf to slope transects were sampled between 150 °W and 151 °W, near the outflow of the Colville River, Alaska (Fig. 1). The 2013 field effort sampled from 13-31 August, during which 47 stations were sampled along six shelf-slope transects between 133 °W and 143 °W, spanning a shelf and slope area from the western Mackenzie shelf and trough in Canada to Camden Bay, Alaska (Fig. 1). All transects ran perpendicular to shore and contained between four to nine sampling stations with target bottom depths of 20, 37, 50, 100, 200, 350, 500, 750 and 1000 m (Table 1). To best characterize the terrestrial matter distribution and trophic structure in the central and eastern Beaufort Sea, transects were grouped into regions based on assumed relative OM_{terr} influence (Dunton et al. 2012) (from east to west): Inner Mackenzie Plume (IMP), Outer Mackenzie Plume (OMP), Camden Bay (CB), and Colville Plume (CP) (Fig. 1). The 20, 37, 50, and 100 m depth stations were considered to represent the Beaufort 'shelf', while deeper stations were considered to represent the 'slope'.

To characterize the large-scale water mass structure at the time of sampling, vertical casts of a SeaBird SBE55 CTD rosette were made to the maximum depth rating of the CTD at each station (500 m in 2012, 600 m in 2013), measuring the potential temperature (°C) and salinity of the water column binned for each meter. These data were later used to plot water mass structure in each region using Ocean Data View (ODV) v.4.5.3 (Schlitzer 2011). To trace the prevalence of Mackenzie River-derived freshwater across the study area during the time of sampling, water samples were collected at each station (2013 only) for oxygen and hydrogen stable isotope

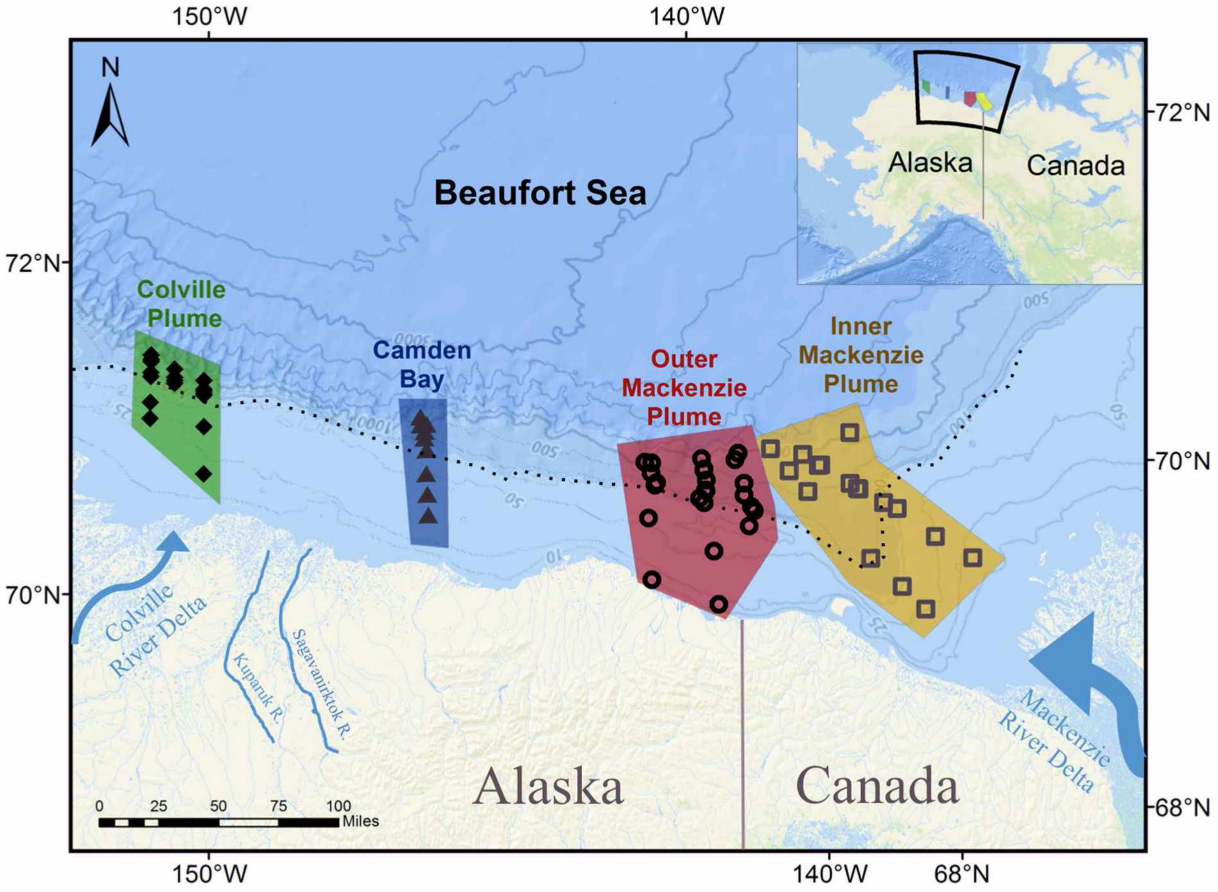

Figure 1. Map of stations sampled in the Beaufort Sea. Colville Plume (CP, ◆) region stations were sampled in Sept 2012, while stations in Camden Bay (CB, ▲), Outer Mackenzie Plume (OMP, ○), and Inner Mackenzie Plume (IMP, □) regions were sampled in Aug 2013. Dotted line indicates Beaufort shelf break at approximately 100 m depth. Ice POM samples were collected from sea ice near Barrow, AK, off map to the west.

Table 1. Station locations and types of isotope samples collected for this study. The majority of samples were collected during the 2012 (Colville Plume [CP] region) and 2013 (Camden Bay [CB], Outer Mackenzie Plume [OMP], and Inner Mackenzie Plume [IMP] regions) field seasons for the BOEM-funded U.S.-Canada Transboundary Project. Stations associated with this project were arranged in transects perpendicular to shore, and have been listed as such here, though transects were pooled for analysis. Additional sPOM samples were collected during the 2013 Canada BREA program (indicated with *), and ice POM samples were collected from sea ice cores outside of Barrow in 2014. Depths listed were target depths, actual sampling depth for bottom trawls was 8.7% less than target depth on average.

Station information							**Isotope samples collected**				
Year	**Region**	**Transect**	**Depth (m)**	**Latitude °N**	**Longitude °W**	**Date sampled**	**Water**	**pPOM**	**sPOM**	**Ice POM**	**Fauna**
2012	**CP**	B2	20	71.0732	-151.1000	28-Sep		x			x
			50	71.1708	-151.1000	28-Sep		x	x		x
			100	71.3261	-151.1000	28-Sep		x			x
			200	71.3502	-151.1000	28-Sep		x			x
			350	71.4167	-151.1000	27-Sep		x			x
			500	71.4297	-151.1000	26-Sep		x			x
			1000	71.4574	-151.1000	26-Sep		x			x
		BX	200	71.2888	-150.6500	29-Sep		x			x
			350	71.3044	-150.6500	29-Sep		x			x
			500	71.3232	-150.6500	29-Sep		x			x
			1000	71.3737	-150.6500	30-Sep		x			x
		B1	20	70.7424	-150.1000	21-Sep		x	x		x
			50	71.0282	-150.1000	21-Sep		x	x		x
			100	71.2167	-150.1000	22-Sep		x			x
			200	71.2301	-150.1000	22-Sep		x	x		x
			350	71.2442	-150.1000	23-Sep			x		x
			500	71.2526	-150.1000	24-Sep		x	x		x
			1000	71.3058	-150.1000	25-Sep		x	x		x
2013	**CB**	A6	20	70.4259	-146.1083	13-Aug	x	x	x		x
			37	70.5500	-146.1006	13-Aug	x	x	x		x
			50	70.6755	-146.0956	13-Aug	x	x	x		x
			100	70.8170	-146.0614	14-Aug	x	x	x		x
			200	70.8902	-146.0812	14-Aug	x	x	x		x
			350	70.9297	-146.0694	15-Aug	x	x			x
			500	70.9704	-146.1313	15-Aug	x	x			x
			750	70.9717	-146.0272	16-Aug	x	x			x
			1000	71.0179	-146.1322	17-Aug	x	x			x
	OMP	A2	10	69.9246	-142.2309	20-Aug	x	x	x		
			40	70.1218	-142.2571	20-Aug	x	x	x		
			100	70.4857	-141.9412	19-Aug			x		
			200	70.4998	-141.9109	19-Aug	x	x	x		
			500	70.5617	-141.9846	19-Aug	x	x			
			750	70.6213	-141.9464	18-Aug	x	x			
			1000	70.6314	-142.0687	18-Aug	x	x			

Table 1 continued.

Station information							Isotope samples collected				
Year	Region	Transect	Depth (m)	Latitude °N	Longitude °W	Date sampled	Water	pPOM	sPOM	Ice POM	Fauna
2013	**OMP cont.**	A1	20	69.7200	-141.1412	20-Aug	x	x	x		x
			50	70.0398	-141.0787	20-Aug	x	x	x		x
			100	70.3379	-141.1176	22-Aug	x	x	x		x
			200	70.3690	-141.1852	22-Aug					x
			350	70.4076	-141.0504	22-Aug	x	x			x
			350	70.4112	-141.0610	5-Sep			x		x
			500	70.4707	-141.0151	22-Aug	x	x			x
			750	70.5321	-141.0347	23-Aug	x	x			x
			750	70.5382	-141.0275	6-Sep			x		x
			1000	70.6027	-141.0407	23-Aug	x	x			x
		TBS	50	70.1562	-140.3967	26-Aug	x	x	x		x
			100	70.2414	-140.2628	25-Aug	x	x	x		x
			200	70.2685	-140.2974	25-Aug	x	x	x		x
			350	70.3449	-140.3903	25-Aug	x	x			x
			500	70.4151	-140.3560	24-Aug	x	x			x
			750	70.5632	-140.4501	24-Aug	x	x			x
			1000	70.5983	-140.3735	24-Aug	x	x			x
	IMP	MAC	50	69.4646	-137.6565	27-Aug	x	x	x		x
			100	69.6281	-137.9703	27-Aug	x	x	x		x
			200	69.8306	-138.4046	26-Aug	x	x	x		x
			500	70.2976	-139.2596	31-Aug	x	x			x
			750	70.4403	-139.5208	31-Aug	x				
			1000	70.5920	-139.7815	30-Aug	x	x			x
		GRY	20	69.7014	-136.6746	27-Aug	x	x	x		x
			50	69.8775	-137.2199	27-Aug	x	x	x		x
			100	70.0920	-137.7705	28-Aug	x	x			x
			200	70.1427	-137.9840	28-Aug	x	x	x		x
			350	70.2532	-138.3628	28-Aug	x	x			x
			350	70.2594	-138.3823	29-Aug			x		x
			500	70.2983	-138.4929	29-Aug	x	x			x
			750	70.4404	-138.9493	29-Aug	x	x			x
			750	70.4409	-138.9866	30-Aug			x		x
			1000	70.5241	-139.2267	30-Aug	x	x			x
		-	1200	70.5980	-138.3180	9-Sep			x		
2014		-	sea ice	71.3815	-156.5243	8-Apr				x	

analysis. Water was collected from the surface and 10 m depth by Niskin bottles attached to the CTD, or surface water was collected with a clean bucket. Each water sample was pipetted into a 2 mL glass vial (Agilent Technologies) with no headspace and crimped closed. These airtight water samples were stored at room temperature until analysis.

At each station in 2012 and 2013, POM was collected from the water column (sub-surface chlorophyll *a* maximum layer, or 20-30 m depth) and from surface sediments (where accessible) to provide baseline values for these potential food resources (e.g., Hobson and Welch 1992; Iken et al. 2005; Dunton et al. 2012). Water samples for pelagic POM (pPOM; n = 3 per station) were collected from Niskin bottles attached to the CTD rosette. Approximately 1 L water for each pPOM replicate was filtered onto a pre-combusted Whatman GF/F filter and frozen at -20 °C until processing for $\delta^{13}C$ and $\delta^{15}N$ value analysis. A single sample of surface sediment POM (sPOM) was taken from the upper 1 cm of a box core (2012) or van Veen grab (2013) at each station where available, placed into a sterile whirl-pak bag and kept frozen until processing for δD, $\delta^{13}C$ and $\delta^{15}N$ value analysis. Additional sediment samples taken from a box core at select 2013 slope stations (n = 5) were provided by the Canadian Beaufort Regional Environmental Assessment (BREA) initiative, as the U.S.-Canada Transboundary cruise was unable to sample surface sediments deeper than 200 m bottom depth in 2013. Sediments from deep stations sampled by BREA were collected within three weeks of the same or nearby stations sampled by the Transboundary project (Table 1).

To investigate marine food web structure across the Beaufort Sea, representative fauna at each station were collected for isotope analysis. Dominant meso-zooplanktonic taxa (Copepoda, Amphipoda, Chaetognatha; n = 3 replicate samples per taxon) were collected whole at each station from 150 μm mesh multinet and 505 μm mesh bongo net deployments. Replicate (n = 3) samples of major benthic invertebrate taxa were collected from van Veen grabs, box cores, beam trawls (4 mm mesh), and otter trawls (19 mm mesh). Collections from trawls also included demersal fish species. Trawls were deployed along the target depth contour within 3.5 km of vertical gear deployed at each shelf station and within 9 km of vertical gear deployed at each slope station. Tissue for isotope analysis was preferentially collected as muscle, but where muscle was inaccessible or insufficient, tissue was also derived from tube feet (Asteroidea), oral discs (Ophiuroidea), body wall (Polychaeta, Echiura, Actinaria), or whole individuals (Amphipoda). When possible, the guts of the whole animals were removed, and all tissues were rinsed with filtered seawater. For smaller pelagic and benthic species, several individuals from the same station were pooled to provide sufficient mass for analysis. Invertebrate tissue samples were frozen onboard at -20 °C and then dried at 60 °C for 24 h. Vouchers of invertebrate taxa of uncertain identification were sent to taxonomic experts for species verification. Fish from beam trawl and bottom trawl catches were identified and frozen on board and muscle tissue from dominant species sampled later (n = 3 replicates per station) for isotope analysis. All taxon names were standardized to the World Register of Marine Species (www.marinespecies.org).

Biomass data for epibenthic invertebrate consumers included in the food web analysis were collected concurrently at each station to quantitatively assess biomass distribution within trophic levels across study regions and depth groups (shelf or slope environments). Invertebrate taxa were quantitatively collected from beam trawl catches, identified on board, and wet weight for each taxon was determined using digital hanging scales. Biomass estimates were calculated from area trawled (= net swath x haul distance) and normalized to 1000 m^{-2}. Beam trawl catches in 2012 (CP region) were deemed non-quantitative and, hence, could not be used for this purpose. Instead, average epibenthic biomass on the CP shelf and upper slope was calculated using data from the 2011 BOEM-funded BeauFish survey, which employed the same trawl type at sites near the 2012 stations, though only to a maximum bottom depth of 200 m (Ravelo et al. in review).

Sea ice algae can be an important food source in Arctic systems (McMahon et al. 2006; Roy et al. in review); however, the sampling cruises for this study occurred during the ice-free summer period. To include an endmember reference value in the trophic mixing models for sea ice algae, ice POM (iPOM) was collected off the northwest coast of Barrow, AK at 71.3815 °N, 156.5243 °W on 8 April 2014 to analyze for $\delta^{13}C$ and $\delta^{15}N$ values. Fist-sized pieces of ice (n = 2) were taken from the bottom of ice cores, placed in ziploc bags and frozen in the field.

Lab processing and stable isotope analysis

At the University of Alaska Fairbanks (UAF), pPOM filters were dried for 24 h at 60 °C, fumed with HCl vapors for 24 h to remove carbonate, and dried again at 60 °C. sPOM samples were thawed, and 1 mL of each sample was repeatedly treated with approximately 6 mL of 1 N HCl until all bubbling ceased to ensure removal of all carbonates (Iken et al. 2010; Goñi et al. 2013). Sediment samples were then rinsed with deionized water until pH stabilized, and then freeze-dried. Ice pieces for ice-associated production were thawed and centrifuged to concentrate iPOM (n = 3 replicates per ice piece), freeze dried, and the remaining organic material was analyzed for $\delta^{13}C$ and $\delta^{15}N$ values. Organism tissue samples that contained carbonate were treated with 1 N HCl, and then dried for 24 h at 60 °C. Because lipids can be depleted in ^{13}C relative to muscle tissue and significantly confound stable carbon isotope interpretation in animals with large lipid stores (Logan et al. 2008; Mintenbeck et al. 2008), all tissue samples were repeatedly treated with 2:1 chloroform:methanol to remove lipids. Samples were then re-dried for 24 h at 60 °C.

Stable isotope data for all samples were obtained using continuous-flow isotope ratio mass spectrometry (CFIRMS) at the Alaska Stable Isotope Facility (ASIF) at UAF. Water samples from 2013 were measured for $\delta^{18}O$ and δD values. sPOM samples and a selection of the most common benthic invertebrate taxa (n = 4 taxa; *Colus sabini, Cryptonatica affinis, Ophiocten sericeum,* Polynoidae) encountered across the study area and shelf/slope habitat were analyzed for δD values. All pPOM, sPOM, and iPOM samples were measured for $\delta^{13}C$ and $\delta^{15}N$ values. Approximately 0.3 mg dry weight of each homogenized faunal tissue sample was analyzed for $\delta^{13}C$ and $\delta^{15}N$ values. δD and $\delta^{18}O$ values were measured using a pyrolysis-elemental analyzer (ThermoScientific high temperature elemental analyzer - TC/EA) attached via a Conflo IV to an isotope ratio mass spectrometer (IRMS; ThermoFinnigan DeltaV^{Plus}). $\delta^{13}C$ and $\delta^{15}N$ values were measured using a Costech ESC 4010 elemental analyzer interfaced via a Conflo IV with an IRMS (Thermo Finnigan Delta V^{Plus}). Results are expressed as conventional δ notation in parts per thousand (‰) according to the following equation:

$$(1) \qquad \delta\ (‰) = ([R_{sample}/R_{standard}] - 1) * 1000$$

where R is the determined ratio of $n(^{i}\text{Element})/n(^{j}\text{Element})$, abbreviated as $^{18}O{:}^{16}O$, $^{2}H{:}^{1}H$, $^{13}C{:}^{12}C$, or $^{15}N{:}^{14}N$. Standards were Vienna Standard Mean Ocean Water (VSMOW) for δD and $\delta^{18}O$ values, Vienna Pee Dee Belemnite (VPDB) for $\delta^{13}C$ values, and atmospheric N_2 for $\delta^{15}N$ values. Instrument precision at ASIF was < 3.0‰ for δD values, < 0.5‰ for $\delta^{18}O$ values, and < 0.2‰ for both $\delta^{13}C$ and $\delta^{15}N$ values.

Data analysis: δD values

Mackenzie River-derived freshwater has largely been characterized by its $\delta^{18}O$ value (Krouse and Mackay 1971; Macdonald et al. 1989; Cooper et al. 2005, 2008; Lansard et al. 2012), but oxygen and hydrogen stable isotopes are known to fractionate synchronously in meteoric water

(Craig 1961). As δD values are a better tracer of organic matter provenance than $\delta^{18}O$ values (Soto et al. 2013), δD isotopic ranges of water, POM and lower trophic level consumer tissue were of greater interest than $\delta^{18}O$ for this study. To determine if $\delta^{18}O$ and δD values of water samples taken in the Beaufort Sea could be used interchangeably as water mass tracers, the relationship between the two stable isotope ratios was compared to that of the Global Meteoric Water Line (GMWL), which describes the predictable association between the $\delta^{18}O$ and δD values of precipitation worldwide (Craig 1961). The interdependence of water sample $\delta^{18}O$ and δD values was tested using a Spearman's rank correlation. Then, the 95% confidence interval of the slope of a linear regression between the two stable isotope ratios was compared to the slope of the GMWL to confirm that they overlapped. Based on the GMWL equation (Craig 1961), the Mackenzie River water δD value was -143.6‰ (Cooper et al. 2008). Assuming near-surface (≤20 m) Beaufort Sea water is a mixture of sea ice melt and the polar mixed layer (Lansard et al. 2012), the ocean-water δD value was specified as approximately -10‰ (Macdonald et al. 1995). Trends in surface and 10 m depth water δD values across the study area were visualized in ODV v.4.5.3 (Schlitzer 2011). For additional verification that water sample δD values were related to freshwater influence, the correlation between water sample salinity and δD values at surface and 10 m depth was tested using Spearman's rank correlation. Predictive relationships between water δD values and longitude or log-transformed station bottom depth were tested using regression analyses ($\alpha = 0.05$).

Published data that could be used to define δD values of terrestrial and marine organic matter endmembers relevant to this study area are very sparse. The mean hydrogen isotope discrimination (ΔD) between phytoplankton and the water they grow in is around -173‰ ± 26‰ (Hondula et al. 2014), though this estimate only considers freshwater phytoplankton from rivers and lakes. Assuming that marine primary production in Arctic Ocean takes place in water with an approximate δD value of -10‰ (Macdonald et al. 1995), the marine organic matter endmember could then be -183‰ ± 26‰. In contrast, mean ΔD between terrestrial plants and groundwater is around -85‰ ± 19‰ (or -82‰ ± 10‰ for *Sphagnum* spp., a major component of Arctic peat (Gajewski et al. 2001)). δD values of precipitation in the Arctic and subarctic vary widely throughout the year (Global Network for Isotopes in Precipitation database, http://isohis.iaea.org, 2014), so an approximation of the δD value of groundwater available to terrestrial plants, the origin of OM_{terr} released into the Beaufort Sea, likely is the composite δD value of freshwater from major Arctic rivers of this region. Assuming the Mackenzie River is the dominant vector of OM_{terr} to the Beaufort, this river's freshwater δD value of -143.6‰ (Cooper et al. 2008) could result in an average terrestrial production endmember δD value of -229‰ ± 19‰. However, the latitudinal extent of the Mackenzie River drainage basin collects meteoric water with higher composite δD values than smaller, higher-latitude Arctic rivers (Hitchon and Krouse 1972; Cooper et al. 2005), so OM_{terr} carried into the Beaufort Sea via smaller rivers or coastal erosion could therefore be expected to have even lower δD values than Mackenzie-derived OM_{terr}. Thus, given the potentially high variability in the δD value of OM_{terr} entering the Beaufort Sea, δD values of sPOM and benthic consumer tissue were considered and interpreted conservatively.

The depth distribution and relative assimilation of OM_{terr} was investigated across the study area by assessing the relationships between bottom depth and sPOM δD values and between bottom depth and benthic consumer δD values by region using regression analysis. Benthic consumer taxa were chosen for δD value analysis based on their presence across longitudinal regions and shelf or slope depth groups. Regression analysis was used to test the predictive relationship between surface water δD values and sPOM δD values, as well as sPOM δD values and benthic consumer δD values at each station by region.

Data analysis: $\delta^{13}C$ and $\delta^{15}N$ values

The terrestrial versus marine composition of pPOM and sPOM samples was determined by comparing their $\delta^{13}C$ and $\delta^{15}N$ values to relatively well-established carbon and nitrogen isotope means of POM endmembers from possible origins: terrestrial POM ($\delta^{13}C$ = -28.8‰ ± 3.2‰, $\delta^{15}N$ = 0.8‰ ± 1.0‰ (Schell et al. 1984; Goñi et al. 2000; Dunton et al. 2006)), marine phytoplankton POM ($\delta^{13}C$ = -24.0‰ ± 0.4‰, $\delta^{15}N$ = 7.7‰ ± 0.3‰, (McTigue and Dunton 2013)), and ice POM ($\delta^{13}C$ = -21.6‰ ± 0.5‰, $\delta^{15}N$ = 8.1‰ ± 4.2‰, this study). The three organic matter sources listed above were used in mixing models using Stable Isotope Analysis in R (SIAR) v.4 (Parnell et al. 2010) to assess their contributions to pPOM and sPOM samples in this study. Terrestrial POM, as mentioned above, reflects a mixture of Mackenzie River POM composed of freshwater aquatic producers and ancient and modern terrestrial plant production from across the Mackenzie River watershed (Goñi et al. 2005), as well as terrestrial peat and tundra plants in the coastal Alaskan Beaufort, which constitute a large part of erosional small river inputs (Schell et al. 1984; Dunton et al. 2012). While both the Mackenzie River and coastal erosion are distinct vectors for OM_{terr} usable by marine consumers to enter the Beaufort Sea (Dunton et al. 2006; Casper et al. 2014), sufficient isotopic resolution to differentiate these two sources of OM_{terr} was not possible in this study. Mixing model calculations assumed no enrichment of pPOM or sPOM isotope values from source endmember values. pPOM and sPOM $\delta^{13}C$ and $\delta^{15}N$ values were analyzed for significant differences among longitudinal regions and between shelf or slope depth groups using two-way analysis of variance (ANOVA, $\alpha = 0.05$), followed by Tukey's post-hoc tests for differences among groups (R 3.0.3; R Development Core Team 2014).

Given the large increase in Arctic ice algal $\delta^{13}C$ values over the growth season at biomass-rich locations from approximately -25‰ in early spring to -14‰ at peak algal production (Tremblay et al. 2006; Gradinger 2009; Gradinger et al. 2009), the temporally-limited endmember isotope ratio used for iPOM in this study may not fully represent the $\delta^{13}C$ range of ice algae present in pPOM and sPOM samples. Unfortunately, published estimates of ice algal $\delta^{13}C$ values specific to the Beaufort shelf and slope region are sparse (i.e., limited to the far western Beaufort; Gradinger 2009). Thus, it was assumed that the $\delta^{13}C$ values of the iPOM sampled for this study in April represented the early growth season and thus lower end of possible iPOM $\delta^{13}C$ values. As a purely exploratory measure, mixing model analysis was also performed using a hypothetical iPOM endmember $\delta^{13}C$ value of -15.5‰ ± 0.8‰ (Gradinger et al. 2009), as a means of theorizing how higher ice algal $\delta^{13}C$ values would alter the relative contributions of organic matter sources to pPOM and sPOM samples.

To investigate how station bottom depth affected pPOM and sPOM composition, the depth-averaged total organic carbon to total nitrogen (C:N) ratios, and $\delta^{13}C$ and $\delta^{15}N$ values of pPOM and sPOM samples were correlated with station bottom depth within regions. Along with $\delta^{13}C$ and $\delta^{15}N$ values, C:N ratios can be an effective proxy for the terrestrial versus marine origins of organic matter, as the atomic C:N ratios of terrestrial plants are typically > 15, whereas phytoplankton atomic C:N ratios range between 4 and 10 (Meyers 1997; Macdonald et al. 2004). Although $\delta^{15}N$ and C:N ratios of organic matter are much more susceptible to alteration during biogeochemical processing than $\delta^{13}C$ values (Thorton and McManus 1994), the simultaneous application of all three organic tracers can provide the strongest indication of the source and alteration history of POM samples.

To confirm that certain species could be grouped at a higher taxonomic level to maximize spatial coverage for comparative purposes (not all taxa occurred at all stations or at the same species level), taxonomic surrogacy was tested between select species at stations where these species co-occurred using Student's t-tests ($\alpha = 0.05$). If two species' isotope values were statistically identical when compared at the same station, these species were considered isotopically equivalent and grouped at their lowest shared taxonomic level. Grouping typically occurred at the shared genus level, though in the most extreme instance grouping was necessary at the shared class level (Pycnogonida). Though aggregation of taxonomic units can affect estimated food web length (Hall and Raffaelli 1991), applying consistent taxonomic levels to make relative comparisons of food web lengths only within this study area is useful.

To discern regional differences in carbon source utilization, $\delta^{13}C$ values of consumers were grouped by feeding guild and analyzed for significant differences between fixed factors region and depth group (shelf or slope) using a two-way ANOVA ($\alpha = 0.05$), and then tested for differences between factor groups using Tukey's post-hoc tests. Taxa were assigned to one of six feeding guilds: pelagic filter feeders (pFilt, n = 3 taxa), pelagic predators (pPred, n = 2), benthic sub-surface deposit feeders (SSDF, n = 3), benthic surface deposit feeders (SDF, n = 9), benthic suspension feeders (Sus, n = 6), and benthic predators or scavengers (Pred, n = 26) based on literature listed in Table 2. The impact of depth on trophic enrichment of $\delta^{15}N$ (Mintenbeck et al. 2007) in benthic consumers was tested with regression analysis of the relationship between benthic consumer $\delta^{15}N$ value and bottom depth. The majority of taxa did not occur across all depths; thus, only some of the most widespread benthic consumers (*Colus sabini, Crossaster papposus, Ophiocten sericeum*, Polynoidae) were chosen for this regression analysis.

Food web length was determined by assuming an average 3.4‰ increase in $\delta^{15}N$ values per trophic level (TL) (Vander Zanden and Rasmussen 2001; Post 2002b). Trophic levels in the overall food web are classified as discrete steps, such as TL 1, TL 2, TL 3, etc. In contrast, the individual trophic position (TP) of each consumer is a continuous variable calculated based on its isotopic distance to a chosen base reference. Particulate organic matter from the subsurface chlorophyll maximum layer or upper 50 m of the water column (pPOM) has been frequently used as a trophic baseline in the analysis of Arctic marine food webs (Hobson et al. 2002; Søreide et al. 2006; Iken et al. 2010). Average pPOM $\delta^{15}N$ values from shelf and slope depth groups by region were used as the base of each food web (pPOM = TL 1) so that the trophic position of each taxon was calculated from the following equation:

(2) $$\mathrm{TP}_{\mathrm{consumer}} = ([\delta^{15}\mathrm{N}_{\mathrm{consumer}} - \delta^{15}\mathrm{N}_{\mathrm{pPOM}}]/3.4) + 1$$

Recent studies have indicated that a depth-stratified approach to defining a baseline is critical when comparing benthic food webs over considerable water depths (Bergmann et al. 2009; Roy et al. in review). Particularly given the steep bathymetry of the Beaufort slope and the complex hydrodynamic processes of the region (Jakobsson et al. 2004; Pickart 2004; Macdonald and Yu 2006; Hwang et al. 2008), near-surface pPOM does not sink entirely vertically and unprocessed through the water column (Forest et al. 2013) to represent organic matter reaching benthic consumers at corresponding deep slope stations. The limited number and lack of replicate sPOM samples prevented their use as a reliable, depth-standardized trophic baseline. Instead, the surface deposit-feeding brittle star *Ophiocten sericeum* was chosen as a primary consumer (PC) baseline. Ideally, use of a PC baseline (e.g., Iken et al. 2010; Roy et al. in review) provides a long-term integration of utilized food sources at the benthos (Vander Zanden and Rasmussen 1999). Due to its facultative feeding style, which allows *Ophiocten* to feed on freshly sedimented organic matter at the benthos when available (Piepenburg 2000), the isotopic values of this brittle star were deemed to be representative of the organic matter sources utilized at any given location. Therefore, as a second approach to food web modeling, *Ophiocten sericeum* was used as a primary consumer common across all stations to calculate trophic positions from the following equation:

(3) $$\mathrm{TP}_{\mathrm{consumer}} = ([\delta^{15}\mathrm{N}_{\mathrm{consumer}} - \delta^{15}\mathrm{N}_{O.\ sericeum}]/3.4) + 2$$

The distribution of benthic biomass across trophic levels is a better indicator of the actual energetic structure of food webs than simply looking at the distribution of taxa across trophic levels. Available epibenthic biomass data (Ravelo et al. in review, for 2012 CP region; Iken and Bluhm unpublished data, for 2013 regions) were used to examine quantitative properties of benthic food web structure to infer on the quality of $\mathrm{OM}_{\mathrm{terr}}$ as a food source to marine communities on the Beaufort shelf and slope. Relative consumer biomass represented within each trophic level was derived from community biomass estimates from trawl catches and compared among food webs by region and shelf or slope depth group. Taxon TP was rounded to the next lowest or highest food web TL, for example such that food web TL 3 category included consumers with TP 2.5 to 3.4, and TL 1 contained all TP < 1.4. Biomass data were not available for all taxa included in the food web analysis, e.g., for infaunal taxa and zooplankton. Thus, only 37 of the 49 taxa included in the full isotopic analysis could be used for this quantitative trophic level biomass comparison. The percentage of total epifaunal biomass represented by the biomass-based TL comparison was noted as a way of indicating the quantity of the missing biomass not analyzed for TP. To ensure that this subset of taxa represented an equivalent trophic structure to the full set of taxa used in the food web analyses, histograms of number of taxa binned by TL were also compared between the full taxon set and the subset, and were found to be comparable (Appendix A).

Results

Large-scale water mass structure

Temperature and salinity profiles averaged across transects within regions (Fig. 2) indicated largely similar vertical water mass structure across the study area. A relatively warm (> 2 °C) and fresh (salinity < 28) surface layer overlaid the very cold (-2 °C) and slightly more saline (28-34) polar mixed/upper halocline layers (see study area description). Off-shelf, at 150 to 200 m water column depth, a distinct thermocline transitioned to warmer (≥ 0 °C) Atlantic water. The OMP region was distinct in that its nearshore surface waters were colder and more saline than were observed in other regions, while the CP region was distinguished from more eastern regions by relatively colder and more saline surface waters and a shallower Atlantic layer.

The δD and $\delta^{18}O$ values of surface and 10 m depth water in the eastern Beaufort Sea (2013) were highly correlated ($R^2 = 0.98$; Fig. 3). The slope of the linear regression between water sample $\delta^{18}O$ and δD values had a confidence interval ($\alpha = 0.05$) that overlapped with the slope of the GMWL. Therefore, there was no transformative fractionation between $\delta^{18}O$ and δD values of surface and 10 m depth water in the eastern Beaufort, confirming the isotope ratio of either element as a water mass tracer. Hereafter, water samples will be characterized only using their δD values. Water δD values from both surface and 10 m depth were highly correlated with salinity ($R^2 = 0.95$), with slight deviations likely due to isotopic fractionation during ice formation and thaw (O'Neil 1968; Macdonald et al. 1995).

Surface water δD values were lowest (~ -100‰) near the Mackenzie River outflow, indicating highest riverine freshwater content, and generally were higher with increasing distance from the Mackenzie River delta (Fig. 3A). Grouping all 2013 regions together, neither longitude nor position over the Beaufort shelf and slope (approximated by station bottom depth) were significant predictors of surface water δD values ($p > 0.05$). However, when grouped by region, station bottom depth was a significant predictor of surface water δD values ($p < 0.01$) in both the IMP and OMP regions (Fig. 4). Shallower stations closer to shore were associated with lower surface water δD values between -100 to -80‰ in the IMP ($R^2 = 0.57$), while they were associated with higher surface water δD values between -80 to -40‰ in the OMP ($R^2 = 0.68$). Farther to the west, in the CB region, there was no relationship between station bottom depth and surface water δD values, which were around -50 to -40‰ throughout. At 10 m depth, the water

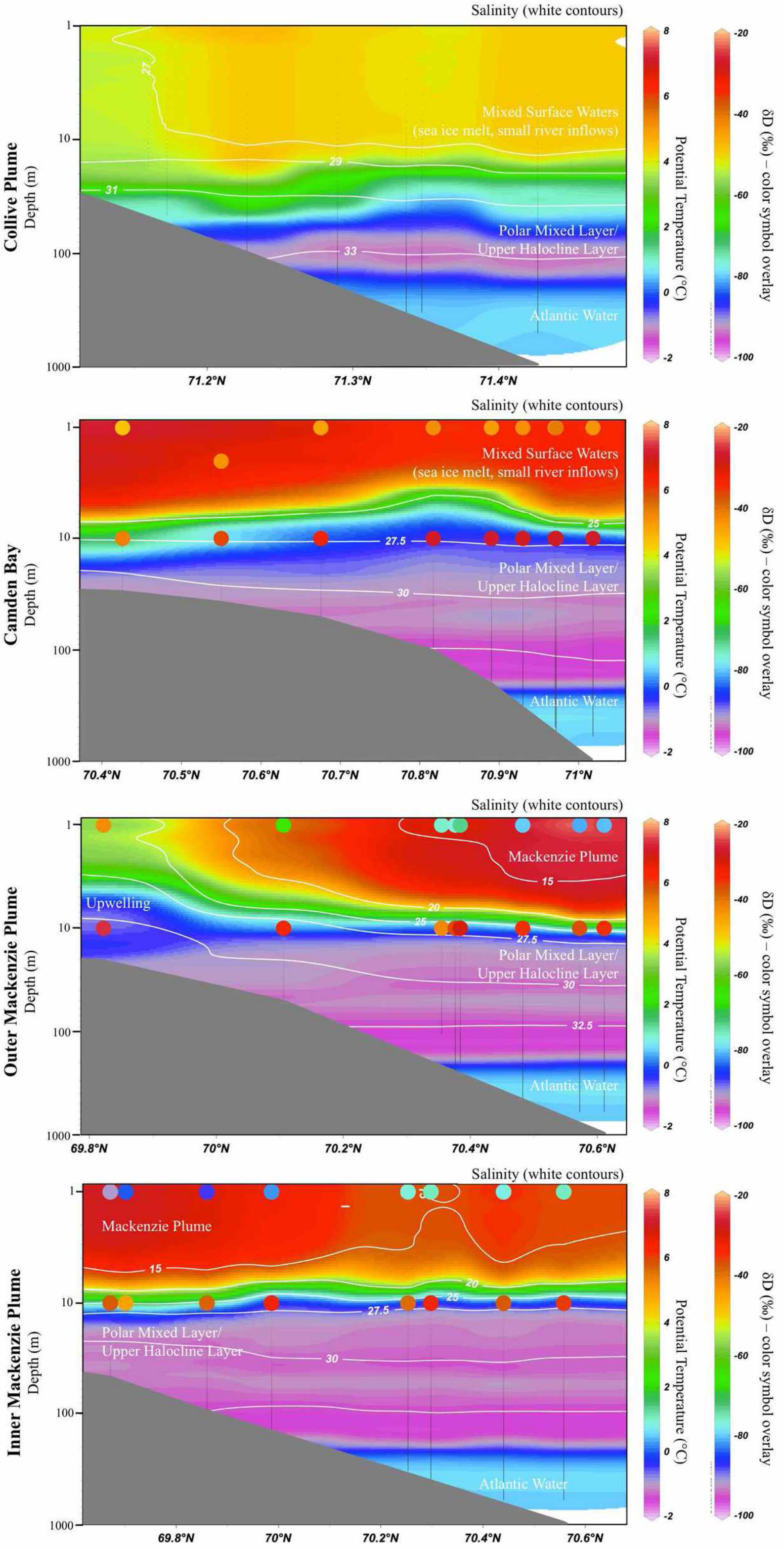

Figure 2. Regionally averaged vertical sections of water temperature, salinity, and δD values. Temperature is indicated by a color gradient with isohaline contours overlaid in white. δD values of water samples from surface and 10 m depth are indicated by color-coded, overlaid circles. Note that depth is on a log scale, and latitudinal scales approximate those of assigned regions.

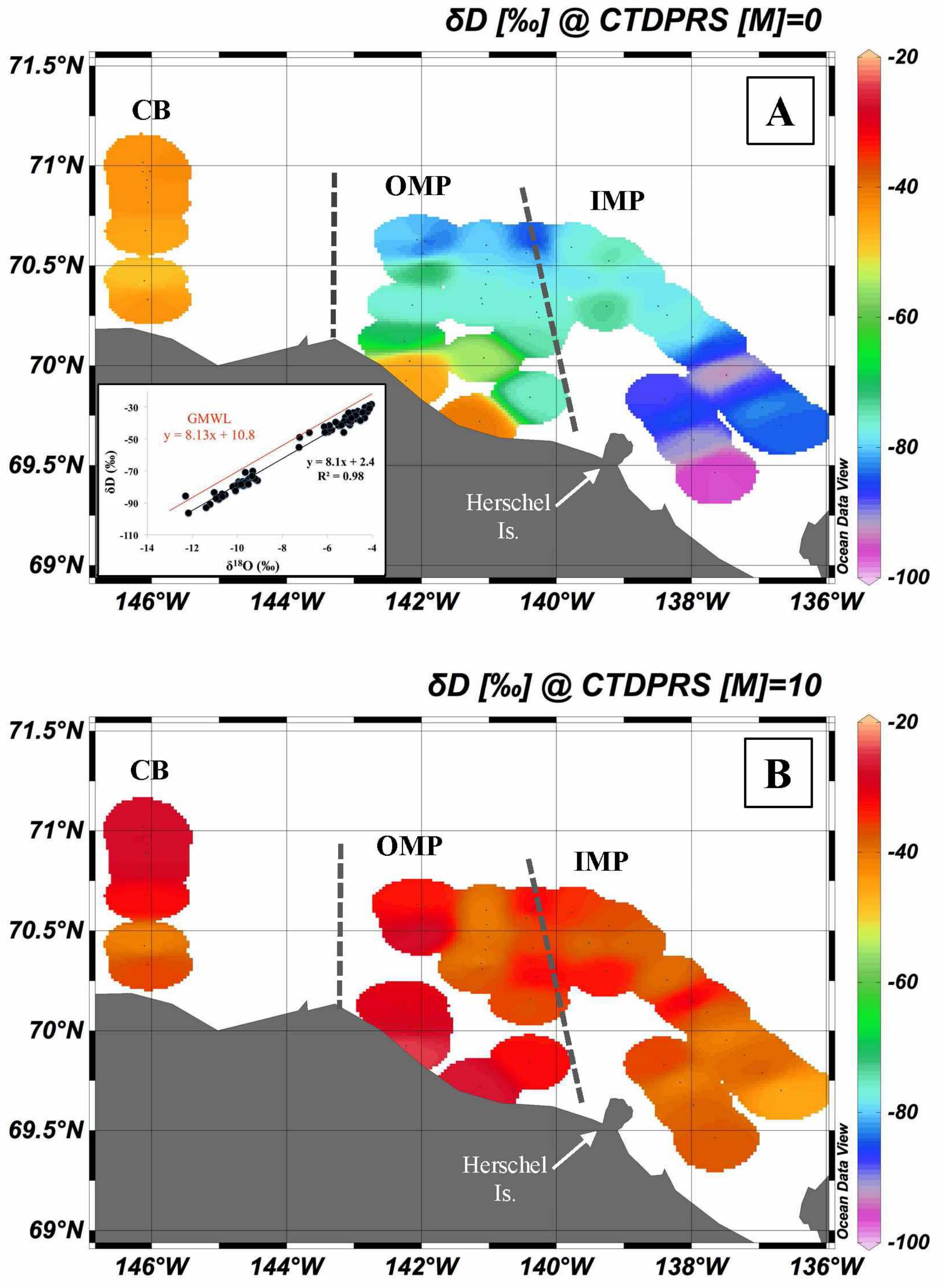

Figure 3. δD values (‰) of water samples taken from the surface (**A**) and 10 m depth (**B**) in the 2013 sampling area (CB, OMP, and IMP regions). The Mackenzie River Delta is to the bottom right corner of the maps. Known δD value of undiluted Mackenzie River water is around -143.6‰, while near surface Beaufort Sea water in this area has a δD value around -10‰ (Macdonald et al. 1995; Cooper et al. 2008). Inset in first panel shows $\delta^{18}O$ vs. δD plot of all surface and 10 m depth water samples, as well as the Global Meteoric Water Line (GMWL) for comparison.

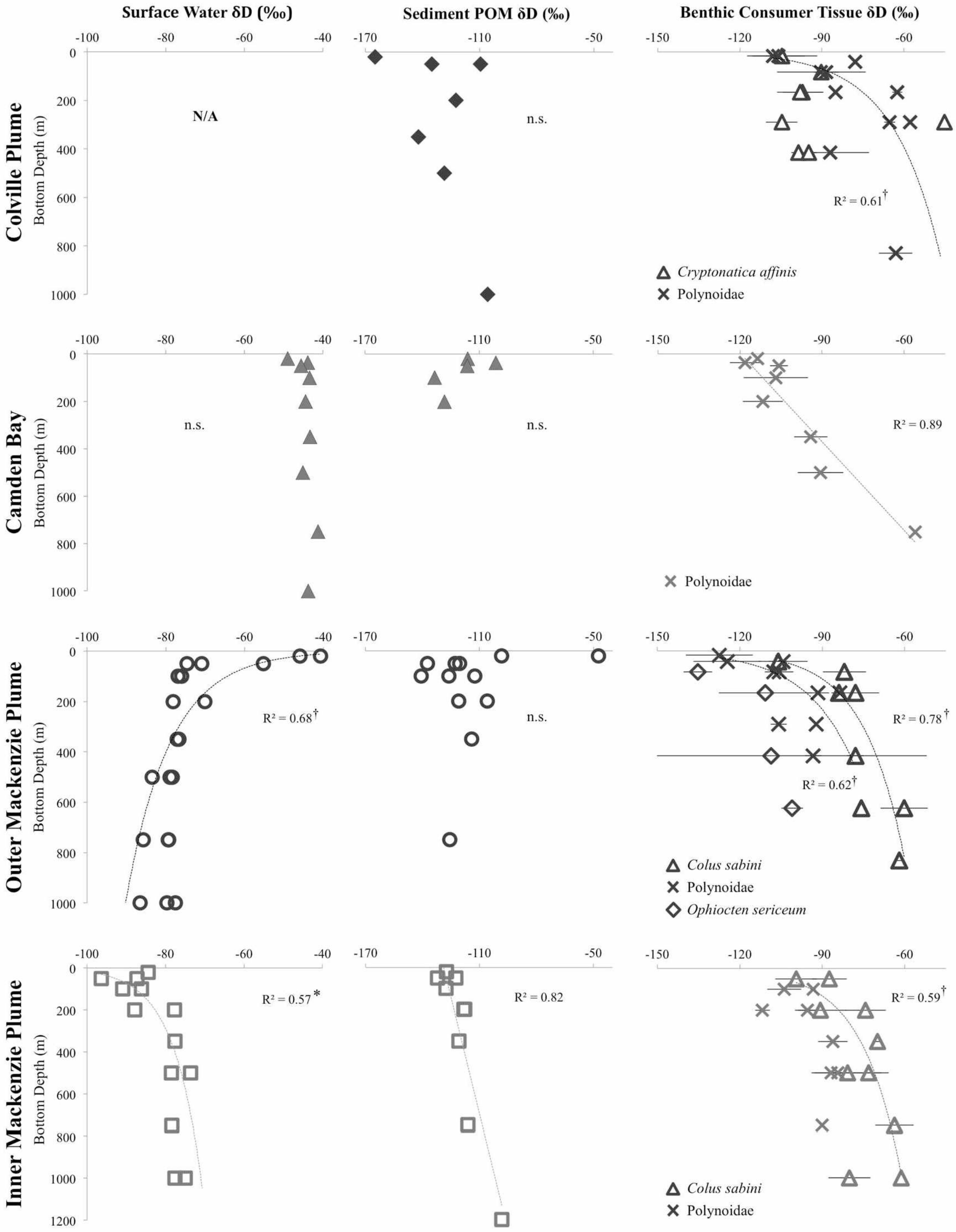

Figure 4. Trends in δD values of surface water, sediment particular organic matter (sPOM), and selected benthic consumers by bottom depth in each region of the Beaufort Sea. Surface water and sPOM data points represent one sample taken at one location, while consumer data represent averages of within-station replicates, with error bars indicating standard deviations. Trend lines and R^2 values are only shown for significant linear relationships between δD data and depth, δD data and $\log_{10}$(depth) (†), or $\log_{10}$(δD data) and $\log_{10}$(depth) (*). All data are shown on non-log scales for comparison.

δD value isoscape was enriched in deuterium relative to the surface and nearly homogenous between -45 and -25‰ across the eastern Beaufort Sea (Fig. 3B), with no relationship between longitude or station bottom depth at a regional level.

Spatial distribution and influence of terrestrial organic matter

sPOM δD values were significantly predicted by bottom depth in the IMP region ($R^2 = 0.82$; $p < 0.001$), with sPOM δD values becoming heavier with increasing bottom depth (Fig. 4). Surface water δD values were only a moderate ($R^2 = 0.61$) although significant ($p < 0.05$) predictor of sPOM δD values in the IMP region. In the OMP, CB, and CP regions, neither bottom depth (Fig. 4) nor surface water δD values were significant predictors of surface sPOM δD values. δD values of Polynoidae were significantly predicted by bottom depth across all regions ($p < 0.001$) except the IMP, with regression analysis indicating a strong positive relationship in CB ($R^2 = 0.89$) and moderate positive relationships in CP ($R^2 = 0.61$) and OMP ($R^2 = 0.62$) (Fig. 4). δD values of predatory gastropods *Colus sabini* and *Cryptonatica affinis*, and surface deposit-feeding *Ophiocten sericeum* also had significant positive relationships ($p < 0.001$) with bottom depth across all regions (range $R^2 = 0.65$ to 0.85). Invertebrate tissue δD values were not significantly predicted by δD values of sPOM samples collected from the same station.

pPOM and sPOM $\delta^{13}C$ and $\delta^{15}N$ values (Table 2) generally fell in between published isotopic values of terrestrial and marine organic matter endmembers, though several samples were outside of the standard deviations of these endmembers (Fig. 5). Across the entire study area, pPOM was composed of an estimated 58% marine POM and 39% terrestrial POM, with only 3% contribution by ice algal POM. In contrast, endmember contributions to sPOM samples were estimated to be more evenly distributed, with 33% from marine POM, 31% from terrestrial POM, and 36% from ice algal POM (when applying the measured iPOM $\delta^{13}C$ and $\delta^{15}N$ values from Barrow). When a more enriched ^{13}C value for iPOM (from May 2003 in Barrow, Gradinger et al. 2009) was used in mixing model analysis, contributions from ice algal POM dropped significantly to 1% in pPOM and 10% in sPOM, while marine POM contributions increased to 60% in both pPOM and sPOM.

The C:N, $\delta^{13}C$, and $\delta^{15}N$ ratios of pPOM and sPOM grouped by region had no significant relationship ($p < 0.05$) with bottom depth (Fig. 6), except for sPOM in the IMP region ($R^2 = 0.81$). $\delta^{13}C$ and C:N values of pPOM and sPOM were not significantly correlated. When depth

Table 2. Mean δ^{13}C and δ^{15}N values (‰) of pPOM, sPOM, and sampled taxa by region and depth group (shelf or slope). Trophic positions (TP) were calculated using the primary consumer baseline. Definitions of feeding guild abbreviations described in methods, and references for each taxon are superscripted and listed below as a footnote. N represents number of samples analyzed in each category.

	Region	**CP**								**CB**							
		Shelf				**Slope**				**Shelf**				**Slope**			
Species/taxon	**Feeding guild**	**δ^{13}C ± sd**	**δ^{15}N ± sd**	**N**	**TP**	**δ^{13}C ± sd**	**δ^{15}N ± sd**	**N**	**TP**	**δ^{13}C ± sd**	**δ^{15}N ± sd**	**N**	**TP**	**δ^{13}C ± sd**	**δ^{15}N ± sd**	**N**	**TP**
pPOM		-25.2 ± 0.5	6.1 ± 1.7	18		-25.6 ± 0.5	6.3 ± 1.3	33		-26.3 ± 1.0	5.8 ± 1.9	12		-26.9 ± 0.9	4.7 ± 1.0	15	
sPOM		-25.4 ± 0.6	4.9 ± 1.6	4		-24.3 ± 0.5	5.4 ± 0.7	7		-21.6 ± 3.9	4.7 ± 1.5	5		-24.5	4.0	1	
ANNELIDA																	
Clitellata																	
Hirudinea	Pred[1]																
Echiura																	
Hamingia arctica	SSDF[2]					-16.7 ± 0.9	14.1 ± 0.9	13	**2.0**								
Polychaeta																	
Nephtys sp.	Pred[1]	-18.9 ± 0.5	13.3 ± 1.6	10	**2.1**	-17.9 ± 0.9	15.3 ± 1.2	6	**2.4**	-20.4 ± 0.4	14.8 ± 1.1	6	**4.3**	-19.6 ± 0.4	16.6 ± 0.8	11	**3.8**
Polynoidae spp.	Pred[1]	-19.2 ± 0.5	13.4 ± 1.2	10	**2.1**	-18.7 ± 0.7	16.0 ± 1.4	14	**2.6**	-20.6 ± 1.0	14.6 ± 1.5	9	**4.3**	-20.5 ± 0.5	16.8 ± 1.1	10	**3.8**
ARTHROPODA																	
Amphipoda																	
Anonyx sp.	Pred[1]	-20.3 ± 0.6	15.0 ± 1.2	16	**2.5**	-20.4 ± 0.8	16.4 ± 1.0	7	**2.7**	-21.0 ± 0.4	13.1 ± 1.9	9	**3.8**	-20.6 ± 0.4	15.7 ± 2.7	10	**3.5**
Themisto libellula	pPred[3]	-22.3 ± 0.7	12.2 ± 0.6	12	**1.7**	-22.1 ± 1.1	12.2 ± 0.7	28	**1.5**	-25.1 ± 0.8	10.0 ± 1.0	9	**2.9**	-24.6 ± 0.9	11.1 ± 1.4	12	**2.2**
Calanoida																	
Calanus glacialis	pFilt[4]	-22.4 ± 0.6	11.2 ± 0.6	15	**1.4**	-21.4 ± 0.7	11.5 ± 0.6	21	**1.3**								
Calanus hyperboreus	pFilt[4]									-23.6 ± 0.8	9.4 ± 1.4	7	**2.7**	-23.7 ± 0.6	10.0 ± 0.8	9	**1.8**
Neocalanus cristatus	pFilt[4]					-22.5 ± 0.4	8.6 ± 0.9	12	**0.4**								
Cumacea																	
Diastylis sp.	SDF[1,2]	-23.1 ± 0.8	8.1 ± 1.0	11	**0.5**	-22.4	8.6	1	**0.4**	-23.6 ± 0.7	5.6 ± 0.9	10	**1.6**	-24.0 ± 0.7	6.2 ± 2.0	4	**0.7**
Decapoda																	
Chionoecetes opilio	Pred[1]					-19.1 ± 0.5	15.7 ± 0.6	14	**2.5**					-18.1	14.6	1	**3.2**
Eualus gaimardii	Pred[1]	-19.7 ± 0.9	14.3 ± 0.7	15	**2.3**	-18.3 ± 1.2	16.0 ± 1.1	23	**2.6**	-19.6 ± 0.5	12.7 ± 0.7	8	**3.7**	-17.7 ± 1.6	15.3 ± 1.2	10	**3.4**
Sabinea septemcarinata	Pred[5]									-18.8 ± 0.5	14.7 ± 0.6	12	**4.3**	-18.4 ± 0.5	15.8 ± 0.8	6	**3.5**
Isopoda																	
Saduria sabini	Pred[6]	-20.2 ± 0.3	13.6 ± 0.1	3	**2.1**	-19.5 ± 0.3	16.9 ± 0.8	9	**2.8**	-22.0 ± 0.4	9.9 ± 1.7	3	**2.9**	-20.5 ± 0.9	13.0 ± 3.1	9	**2.7**
Pycnogonida																	
Pycnogonida	Pred[1]													-21.3 ± 0.2	14.9 ± 0.6	3	**3.3**
CHAETOGNATHA																	
Parasagitta elegans	pPred[7]	-20.0 ± 0.8	15.4 ± 0.6	9	**2.7**	-20.3 ± 0.9	14.9 ± 0.5	31	**2.3**								
CHORDATA																	
Anisarchus medius	Pred[8]																
Aspidophoroides olrikii	Pred[8]	-20.2 ± 0.6	15.6 ± 1.1	9	**2.7**	-19.4 ± 0.6	16.8 ± 0.7	6	**2.8**								
Boreogadus saida	Pred[8]	-21.4 ± 0.4	13.6 ± 0.7	18	**2.1**	-21.4 ± 0.6	13.7 ± 1.2	36	**1.9**	-24.2 ± 0.6	10.4 ± 0.5	3	**3.0**	-22.1 ± 0.7	14.4 ± 1.0	9	**3.1**
Icelus spatula	Pred[8]	-20.3 ± 0.6	15.1 ± 1.3	8	**2.6**					-20.6 ± 0.4	15.1 ± 1.1	3	**4.4**				
Lycodes adolfi	Pred[8]					-19.3 ± 0.4	18.9 ± 0.7	6	**3.4**								
Lycodes seminudus	Pred[8]					-19.0 ± 0.6	18.4 ± 1.0	18	**3.3**								
Triglops pingelii	Pred[8]	-20.0 ± 0.3	14.6 ± 0.6	9	**2.4**	-20.7 ± 1.0	14.5 ± 1.2	4	**2.1**								

Table 2 continued.

	Region	CP								CB							
		Shelf				**Slope**				**Shelf**				**Slope**			
Species/taxon	**Feeding guild**	**δ^{13}C ± sd**	**δ^{15}N ± sd**	**N**	**TP**	**δ^{13}C ± sd**	**δ^{15}N ± sd**	**N**	**TP**	**δ^{13}C ± sd**	**δ^{15}N ± sd**	**N**	**TP**	**δ^{13}C ± sd**	**δ^{15}N ± sd**	**N**	**TP**
CNIDARIA																	
Allantactis parasitica	Sus[9]													-18.4 ± 0.5	16.8 ± 0.8	6	**3.9**
Gersemia sp.	Sus[2]									-21.9 ± 0.1	12.0 ± 0.3	3	**3.5**	-21.8 ± 0.1	15.7 ± 1.0	3	**3.5**
Stomphia sp.	Sus[10]	-17.7 ± 0.6	17.3 ± 0.2	3	**3.2**	-17.9 ± 1.4	18.3 ± 1.2	9	**3.2**								
ECHINODERMATA																	
Asteroidea																	
Ctenodiscus crispatus	SDF[1]	-19.9	15.2	1	**2.6**	-17.7 ± 0.7	17.5 ± 0.7	27	**3.0**	-19.6 ± 0.9	16.0 ± 0.9	3	**4.7**	-19.3 ± 0.5	16.0 ± 1.1	9	**3.6**
Icasterias panopla	Pred[11]																
Pontaster tenuispinus	Pred[12]									-17.8 ± 0.8	16.5 ± 0.8	3	**4.8**	-19.1 ± 0.7	15.8 ± 1.5	13	**3.6**
Bathybiaster vexillifer	Pred[2,13]					-16.7 ± 0.4	21.6 ± 0.7	18	**4.2**								
Crossaster papposus	Pred[1]	-18.2 ± 0.8	19.3 ± 0.8	9	**3.8**	-17.2 ± 1.1	21.0 ± 1.0	20	**4.0**	-20.2 ± 0.8	15.2 ± 1.9	5	**4.5**				
Crinoidea																	
Florometra spp.	Sus[12]																
Holothuroidea																	
Molpadia borealis	SSDF[1,12]					-16.6 ± 0.8	17.5 ± 2.1	3	**3.0**					-18.9 ± 0.8	17.1 ± 2.7	6	**3.9**
Myriotrochus rinkii	SDF[12]	-20.5 ± 1.3	12.1 ± 0.8	9	**1.7**	-20.1 ± 0.4	12.8 ± 0.4	6	**1.6**								
Psolus peronii	Sus[1,12]									-21.8 ± 0.4	9.9 ± 0.5	6	**2.9**				
Ophiuroidea																	
Gorgonocephalus spp.	Pred[1,12]																
Ophiacantha bidentata	SDF[1,12]	-20.4 ± 0.7	17.0 ± 1.0	6	**3.1**	-20.0 ± 0.9	17.5 ± 1.4	6	**3.0**								
Ophiocten sericeum	SDF[1]	-20.9 ± 0.8	13.1 ± 0.3	3	**2.0**	-21.4 ± 1.1	14.1 ± 2.4	3	**2.0**	-22.7 ± 1.5	6.9 ± 3.7	15	**2.0**	-21.7 ± 1.8	10.5 ± 1.7	20	**2.0**
Ophiopleura borealis	SDF[12]					-20.2 ± 1.1	15.4 ± 0.8	8	**2.4**					-17.7 ± 1.7	14.4 ± 0.9	9	**3.1**
Ophiura sarsii	SDF[12,13]	-21.6 ± 0.4	12.4 ± 0.6	9	**1.8**	-21.2 ± 0.6	13.1 ± 0.9	26	**1.7**								
MOLLUSCA																	
Bivalvia																	
Bathyarca glacialis	Sus[2,13]									-20.0 ± 0.5	11.4 ± 0.5	3	**3.3**	-19.8 ± 0.8	12.5 ± 1.7	9	**2.6**
Similipecten greenlandicus	Sus[14]									-19.5 ± 1.7	9.5 ± 1.3	12	**2.8**	-19.0 ± 0.2	13.3 ± 0.3	3	**2.8**
Yoldia hyperborea	SSDF[1]	-21.3 ± 0.2	8.5 ± 0.4	3	**0.6**	-19.5 ± 0.6	8.8 ± 1.8	14	**0.4**								
Cephalopoda																	
Bathypolypus arcticus	Pred	-20.6 ± 0.2	13.8 ± 0.2	3	**2.2**	-18.3 ± 0.7	17.9 ± 0.9	3	**3.1**								
Cirroteuthis sp.	Pred					-20.4	15.7	1	**2.5**								
Gastropoda																	
Buccinum scalariforme	Pred[1]	-19.7 ± 0.8	13.6 ± 0.8	3	**2.1**	-18.5 ± 0.7	15.2 ± 1.9	19	**2.3**	-19.4 ± 1.0	14.2 ± 0.9	3	**4.1**	-16.9 ± 0.4	17.3 ± 0.4	3	**4.0**
Colus sabini	Pred[1]													-18.4	15.3	1	**3.4**
Cryptonatica affinis	Pred[1]	-18.0 ± 0.8	13.5 ± 0.9	5	**2.1**	-17.9 ± 0.6	13.7 ± 1.2	22	**1.9**								
Margarites spp.	SDF[1]	-20.7 ± 0.5	11.8 ± 0.9	7	**1.6**	-20.6 ± 0.4	12.4 ± 0.5	12	**1.5**	-19.8 ± 1.8	9.2 ± 1.1	9	**2.7**				
Tachyrhynchus erosus	Pred[1]					-19.0 ± 2.9	10.5 ± 0.6	21	**0.9**								
Scaphopoda																	
Siphonodentalium sp.	SDF[15]													-17.8 ± 2.7	10.9 ± 2.8	6	**2.1**
PORIFERA																	
Polymastia sp.	Sus[1]	-20.5 ± 0.5	11.1 ± 1.3	3	**1.4**	-20.4 ± 0.7	16.8 ± 1.4	3	**2.8**								

1) Macdonald et al. 2010
2) Bergmann et al. 2009
3) Auel and Werner 2003
4) Mauchline 1998
5) Graeve et al. 1997
6) Haahtela 1990
7) Terazaki 1998
8) Mecklenburg et al. 2002
9) Mercier et al. 2011
10) Lundsten et al. 2010
11) Jangoux and Lawrence 1982
12) Mah 2014
13) Aitken and Fournier 1993
14) Pieńkowski et al. 2014
15) Reynolds 2006

Table 2 continued.

	Region	OMP					
		Shelf				**Slope**	
Species/taxon	**Feeding guild**	**$\delta^{13}C$ ± sd**	**$\delta^{15}N$ ± sd**	**N**	**TP**	**$\delta^{13}C$ ± sd**	**$\delta^{15}N$ ± sd**
pPOM		-26.1 ± 0.8	4.1 ± 2.0	21		-26.7 ± 1.1	4.5 ± 1.5
sPOM		-24.2 ± 1.5	6.1 ± 2.6	8		-24.5 ± 0.7	6.7 ± 2.8
ANNELIDA							
Clitellata							
Hirudinea	Pred[1]						
Echiura							
Hamingia arctica	SSDF[2]						
Polychaeta							
Nephtys sp.	Pred[1]	-21.1	14.3	1	**3.9**	-20.6 ± 0.8	15.5 ± 0.9
Polynoidae spp.	Pred[1]	-21.2 ± 1.1	13.7 ± 1.3	12	**3.7**	-21.4 ± 0.8	15.4 ± 0.9
ARTHROPODA							
Amphipoda							
Anonyx sp.	Pred[1]	-21.4 ± 0.3	12.9 ± 1.8	14	**3.5**	-21.8 ± 0.2	11.0 ± 0.7
Themisto libellula	pPred[3]	-26.5 ± 0.6	10.0 ± 0.8	15	**2.6**	-26.0 ± 0.8	10.1 ± 1.2
Calanoida							
Calanus glacialis	pFilt[4]						
Calanus hyperboreus	pFilt[4]	-24.5 ± 0.5	9.9 ± 0.7	15	**2.6**	-24.4 ± 0.7	9.7 ± 0.7
Neocalanus cristatus	pFilt[4]						
Cumacea							
Diastylis sp.	SDF[1,2]	-23.5 ± 1.3	5.8 ± 0.7	9	**1.4**	-25.7 ± 0.9	5.6 ± 0.9
Decapoda							
Chionoecetes opilio	Pred[1]						
Eualus gaimardii	Pred[1]	-19.8 ± 0.9	13.0 ± 0.6	18	**3.5**	-19.2 ± 1.3	13.9 ± 1.0
Sabinea septemcarinata	Pred[5]	-18.3 ± 1.2	13.9 ± 0.9	15	**3.8**	-18.0 ± 1.3	13.9 ± 0.9
Isopoda							
Saduria sabini	Pred[6]					-22.6 ± 1.7	10.4 ± 2.5
Pycnogonida							
Pycnogonida	Pred[1]	-22.6 ± 0.4	10.2 ± 1.2	10	**2.7**	-22.5 ± 1.1	11.5 ± 1.2
CHAETOGNATHA							
Parasagitta elegans	pPred[7]						
CHORDATA							
Anisarchus medius	Pred[8]						
Aspidophoroides olrikii	Pred[8]	-21.1 ± 0.3	14.4 ± 0.5	6	**3.9**		
Boreogadus saida	Pred[8]	-22.7 ± 0.4	14.0 ± 0.6	11	**3.8**	-24.1 ± 1.8	12.3 ± 2.5
Icelus spatula	Pred[8]	-21.3 ± 0.3	15.2 ± 0.7	12	**4.1**		
Lycodes adolfi	Pred[8]					-20.8 ± 0.7	17.0 ± 0.8
Lycodes seminudus	Pred[8]					-21.1 ± 0.4	16.5 ± 1.1
Triglops pingelii	Pred[8]	-22.2 ± 0.4	13.6 ± 0.4	6	**3.7**	-22.6	15.2

		IMP							
		Shelf				**Slope**			
N	**TP**	**δ^{13}C ± sd**	**δ^{15}N ± sd**	**N**	**TP**	**δ^{13}C ± sd**	**δ^{15}N ± sd**	**N**	**TP**
39		-26.9 ± 0.7	4.3 ± 1.4	15		-26.9 ± 1.0	5.5 ± 2.1	24	
4		-26.0 ± 0.1	4.5 ± 2.2	4		-25.0 ± 0.5	6.7 ± 1.6	5	
						-19.8	16.0 ± 1.5	2	**3.9**
20	**3.7**	-21.9 ± 0.6	13.3 ± 1.0	6	**3.2**	-20.9 ± 0.9	15.1 ± 1.4	11	**3.7**
12	**3.7**	-21.5 ± 1.4	14.0 ± 2.1	11	**3.5**	-21.8 ± 0.7	15.2 ± 1.7	15	**3.7**
2	**2.4**	-21.8 ± 0.5	13.7 ± 1.2	11	**3.4**	-21.4 ± 0.7	14.3 ± 2.6	5	**3.4**
30	**2.1**	-26.8 ± 0.7	10.5 ± 1.2	12	**2.4**	-26.3 ± 0.7	10.3 ± 0.9	24	**2.3**
30	**2.0**	-24.5 ± 0.5	9.4 ± 0.8	12	**2.1**	-24.4 ± 0.5	9.8 ± 0.5	24	**2.1**
17	**0.8**	-24.5 ± 1.8	5.5 ± 1.1	12	**1.0**	-25.5 ± 0.9	5.7 ± 1.1	14	**0.9**
21	**3.2**	-20.9 ± 1.0	12.8 ± 1.0	8	**3.1**	-19.7 ± 1.0	13.9 ± 0.9	19	**3.3**
7	**3.2**	-19.6 ± 0.9	14.0 ± 0.6	13	**3.5**	-19.3 ± 0.5	14.7 ± 1.0	9	**3.6**
17	**2.2**	-22.3 ± 0.6	10.7 ± 1.2	12	**2.5**	-22.6 ± 0.7	10.9 ± 1.3	14	**2.4**
18	**2.5**	-23.0 ± 0.7	11.4 ± 1.6	7	**2.7**	-22.8 ± 0.5	12.9 ± 1.6	20	**3.0**
		-21.9 ± 0.4	14.4 ± 1.0	6	**3.6**				
		-21.5 ± 1.0	14.8 ± 0.9	6	**3.7**				
30	**2.8**	-25.2 ± 1.8	11.5 ± 2.2	12	**2.7**	-24.6 ± 1.6	11.9 ± 2.2	24	**2.7**
		-21.8 ± 0.5	15.4 ± 0.7	9	**3.9**				
9	**4.1**					-21.5 ± 0.8	15.7 ± 2.0	11	**3.8**
12	**4.0**					-21.0 ± 0.5	16.4 ± 0.7	10	**4.1**
1	**3.6**	-22.2 ± 0.7	14.2 ± 0.8	7	**3.5**	-22.2 ± 0.5	14.8 ± 0.8	5	**3.6**

Table 2 continued.

	Region	**OMP**								**IMP**							
		Shelf				**Slope**				**Shelf**				**Slope**			
Species/taxon	**Feeding guild**	**δ^{13}C ± sd**	**δ^{15}N ± sd**	**N**	**TP**	**δ^{13}C ± sd**	**δ^{15}N ± sd**	**N**	**TP**	**δ^{13}C ± sd**	**δ^{15}N ± sd**	**N**	**TP**	**δ^{13}C ± sd**	**δ^{15}N ± sd**	**N**	**TP**
CNIDARIA																	
Allantactis parasitica	Sus[9]	-20.6 ± 0.6	12.4 ± 1.0	4	**3.3**	-18.7 ± 0.8	15.4 ± 1.3	16	**3.7**	-21.1 ± 1.0	13.1 ± 1.2	9	**3.2**	-18.6 ± 1.5	15.8 ± 1.5	17	**3.9**
Gersemia sp.	Sus[2]	-22.4 ± 0.6	10.7 ± 1.8	2	**2.8**	-22.5 ± 0.8	13.5 ± 0.7	9	**3.1**	-23.1 ± 0.9	11.6 ± 0.8	11	**2.7**	-22.5 ± 0.9	12.8 ± 0.8	9	**3.0**
Stomphia sp.	Sus[10]																
ECHINODERMATA																	
Asteroidea																	
Ctenodiscus crispatus	SDF[1]									-20.6 ± 0.8	15.0 ± 1.5	7	**3.7**	-20.1 ± 0.1	15.2 ± 1.7	2	**3.7**
Icasterias panopla	Pred[11]	-19.9 ± 0.3	16.7 ± 0.7	5	**4.6**	-18.9 ± 0.7	18.8 ± 0.6	16	**4.7**	-18.6	17.5	1	**4.5**	-18.8 ± 0.9	18.2 ± 1.3	12	**4.6**
Pontaster tenuispinus	Pred[12]	-19.8 ± 0.4	13.6 ± 0.4	6	**3.7**	-19.5 ± 1.3	15.0 ± 1.3	30	**3.6**	-20.2	15.6	1	**3.9**	-19.3 ± 1.3	14.4 ± 1.5	22	**3.5**
Bathybiaster vexillifer	Pred[2,13]																
Crossaster papposus	Pred[1]	-20.8 ± 0.5	16.0 ± 0.8	10	**4.4**												
Crinoidea																	
Florometra spp.	Sus[12]	-22.9 ± 0.4	12.5 ± 0.4	16	**3.3**												
Holothuroidea																	
Molpadia borealis	SSDF[1,12]					-20.2 ± 0.8	15.2 ± 1.8	9	**3.6**					-19.4 ± 1.0	14.6 ± 1.7	4	**3.5**
Myriotrochus rinkii	SDF[12]																
Psolus peronii	Sus[1,12]	-22.6 ± 0.5	9.9 ± 0.8	9	**2.6**												
Ophiuroidea																	
Gorgonocephalus spp.	Pred[1,12]					-20.5 ± 0.5	16.7 ± 0.3	3	**3.4**	-22.0 ± 0.5	13.9 ± 0.8	8	**4.0**				
Ophiacantha bidentata	SDF[1,12]																
Ophiocten sericeum	SDF[1]	-22.9 ± 2.0	7.9 ± 2.1	25	**2.0**	-22.2 ± 2.2	9.7 ± 0.9	22	**2.0**	-22.9 ± 0.9	9.0 ± 1.0	11	**2.0**	-23.3 ± 0.7	9.4 ± 1.0	7	**2.0**
Ophiopleura borealis	SDF[12]					-17.7 ± 1.6	13.0 ± 1.1	29	**3.0**					-18.4 ± 1.8	12.4 ± 1.6	22	**2.9**
Ophiura sarsii	SDF[12,13]																
MOLLUSCA																	
Bivalvia																	
Bathyarca glacialis	Sus[2,13]	-20.9 ± 0.4	9.9 ± 0.4	8	**2.6**	-20.8 ± 0.5	11.8 ± 1.4	11	**2.6**	-21.6 ± 0.6	9.6 ± 1.0	10	**2.2**	-21.3 ± 0.3	11.9 ± 0.7	12	**2.7**
Similipecten greenlandicus	Sus[14]	-19.7 ± 2.6	9.5 ± 1.0	13	**2.4**					-21.5 ± 1.9	9.7 ± 0.7	12	**2.2**	-22.1	9.8	1	**2.1**
Yoldia hyperborea	SSDF[1]																
Cephalopoda																	
Bathypolypus arcticus	Pred																
Cirroteuthis sp.	Pred																
Gastropoda																	
Buccinum scalariforme	Pred[1]									-20.4 ± 0.9	11.7 ± 2.2	5	**2.8**				
Colus sabini	Pred[1]	-19.8 ± 0.7	12.1 ± 1.3	6	**3.2**	-19.3 ± 1.2	13.8 ± 1.1	16	**3.2**	-20.4 ± 0.7	12.8 ± 1.2	8	**3.1**	-19.5 ± 0.8	14.6 ± 1.9	20	**3.5**
Cryptonatica affinis	Pred[1]																
Margarites spp.	SDF[1]	-21.2 ± 0.9	9.0 ± 1.4	12	**2.3**					-21.4 ± 1.1	9.5 ± 0.8	4	**2.1**	-22.3 ± 0.8	10.1 ± 0.8	6	**2.2**
Tachyrhynchus erosus	Pred[1]																
Scaphopoda																	
Siphonodentalium sp.	SDF[15]					-20.5 ± 2.7	9.9 ± 1.7	16	**2.1**					-20.7 ± 2.5	10.0 ± 0.9	17	**2.2**
PORIFERA																	
Polymastia sp.	Sus[1]	-22.5 ± 1.0	8.3 ± 2.6	3	**2.1**	-21.0 ± 0.4	10.2 ± 1.3	3	**2.1**					-20.7 ± 2.9	8.8 ± 5.2	4	**1.8**

1) Macdonald et al. 2010
2) Bergmann et al. 2009
3) Auel and Werner 2003
4) Mauchline 1998
5) Graeve et al. 1997
6) Haahtela 1990
7) Terazaki 1998
8) Mecklenburg et al. 2002
9) Mercier et al. 2011
10) Lundsten et al. 2010
11) Jangoux and Lawrence 1982
12) Mah 2014
13) Aitken and Fournier 1993
14) Pieńkowski et al. 2014
15) Reynolds 2006

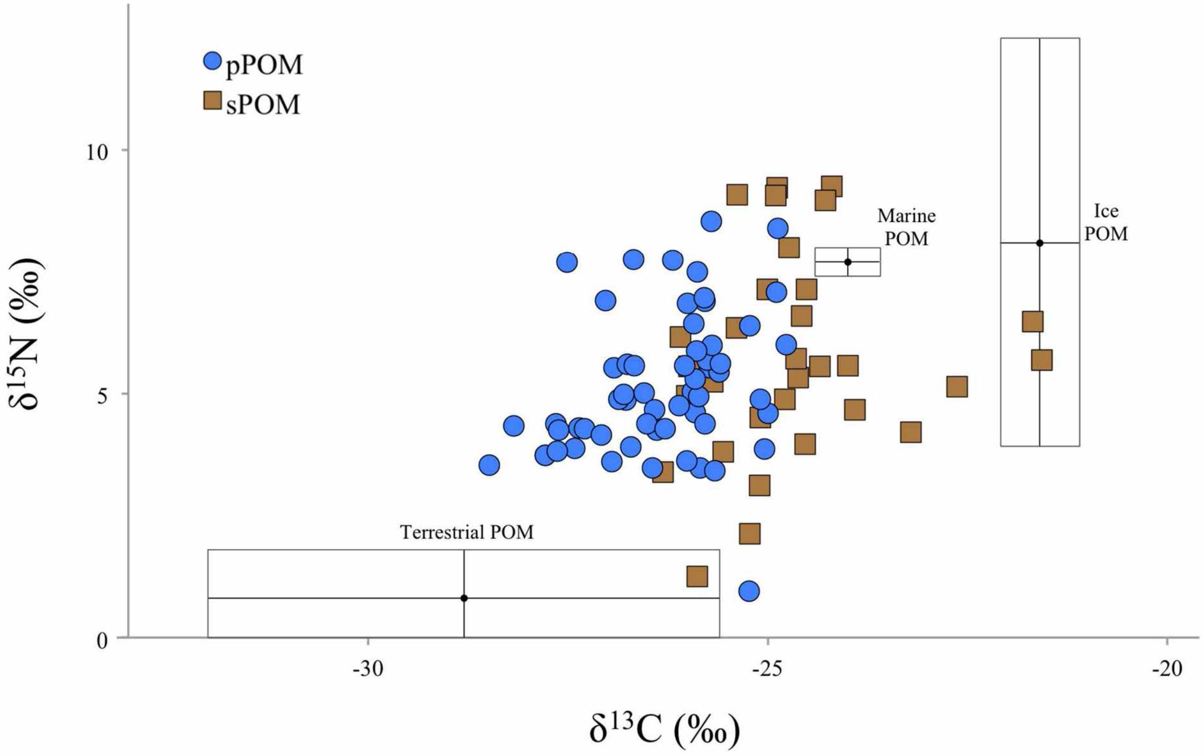

Figure 5. Biplot of $\delta^{13}C$ and $\delta^{15}N$ values for pPOM and sPOM compared alongside potential POM endmembers in the eastern Beaufort Sea. Each pPOM symbol represents a station average of three replicates, while sPOM symbols represent the single sample taken at each station. Boxes encompass standard deviations from the mean isotopic values of each POM endmember (ranges from literature sources, see text for details).

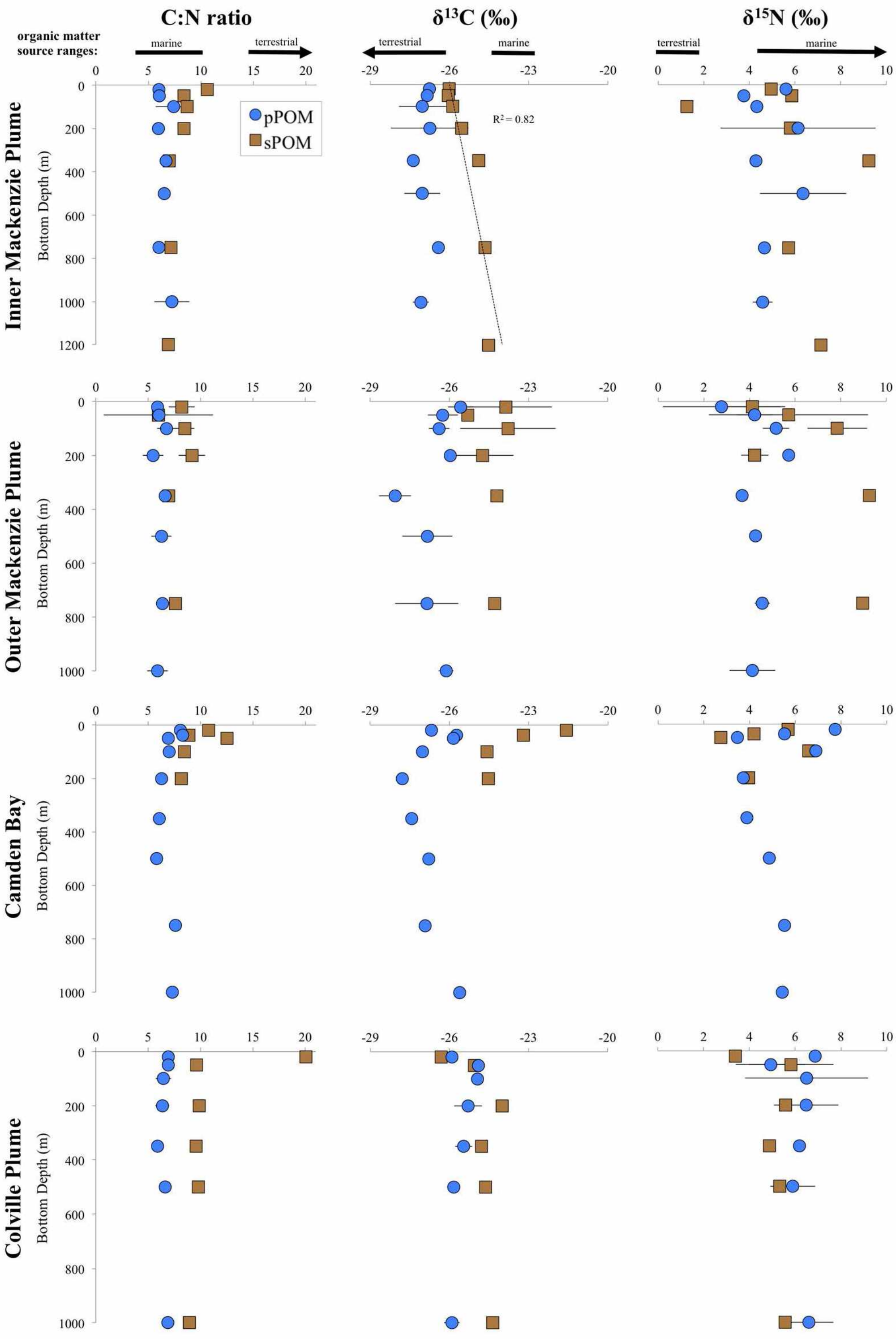

Figure 6. Carbon to nitrogen ratios, δ13C and δ15N values of pPOM and sPOM with station bottom depth, averaged by region. Error bars indicate standard deviation between replicates across transects, and trend lines and R^2 values are only shown for significant relationships between organic matter tracer and station bottom depth. Arrows above the x-axis indicate typical value ranges for terrestrial and marine organic matter based on published literature.

was grouped categorically into shelf versus slope locations, pPOM $\delta^{13}C$ values were significantly affected by both region and depth group (ANOVA, $p < 0.05$), though the interaction between fixed factors region and depth group was not significant. pPOM in the CP region was significantly enriched in ^{13}C compared with more eastern regions over both the shelf and the slope (Fig. 7). In all regions except the IMP, mean pPOM $\delta^{13}C$ values were higher on the shelf relative to the slope; however, these differences were not significant because of high within-region variation. sPOM $\delta^{13}C$ values were significantly lower on the shelf versus slope in the CP and IMP regions, but were not significantly different elsewhere (Fig. 7). sPOM $\delta^{13}C$ values were not well correlated with either pPOM $\delta^{13}C$ or sPOM δD values sampled at the same stations ($R^2 = 0.16$ and 0.28, respectively), undermining the notion of interchangeable use of $\delta^{13}C$ and δD in tracing organic matter provenance. $\delta^{15}N$ values of pPOM and sPOM were not significantly different between shelf and slope stations across or within regions.

Mean $\delta^{13}C$ values of consumers (Table 2) grouped by feeding guild generally decreased when moving eastward from the CP to the IMP region, though the statistical significance of these trends depended on feeding guild and region (Fig. 7). $\delta^{13}C$ values of pelagic filter feeders and pelagic predators in the CP region were significantly (ANOVA, $p < 0.001$) higher compared with these pelagic consumers in all other regions for both shelf and slope depth groups. Benthic predators in both the CP and CB regions were significantly (ANOVA, $p < 0.001$) enriched in ^{13}C compared with predators on the IMP shelf and the OMP and IMP slope. Regional trends in $\delta^{13}C$ values for benthic sub-surface and surface deposit feeders and suspension feeders were not significant. Within-region differences between the shelf and slope did not show a consistent pattern across feeding guilds (Fig. 7).

Regional and depth variation in food web structure

$\delta^{15}N$ values of a selection of the most widespread consumers (*Colus sabini, Crossaster papposus, Ophiocten sericeum,* Polynoidae) from across the study area had significant ($p < 0.001$) positive relationships (R^2 range = 0.45 - 0.66) with bottom depth with an increase in $\delta^{15}N$ values on the order of 2 to 5‰ from 20 to 1000 m (Fig. 8). This overall trend of increasing $\delta^{15}N$ ratios with depth was observed for the majority of benthic taxa and feeding guilds, but could not be statistically confirmed for less widespread taxa. While not significant, there also appeared to be a trend of increased sPOM $\delta^{15}N$ values with bottom depth in the IMP and OMP regions (Fig.

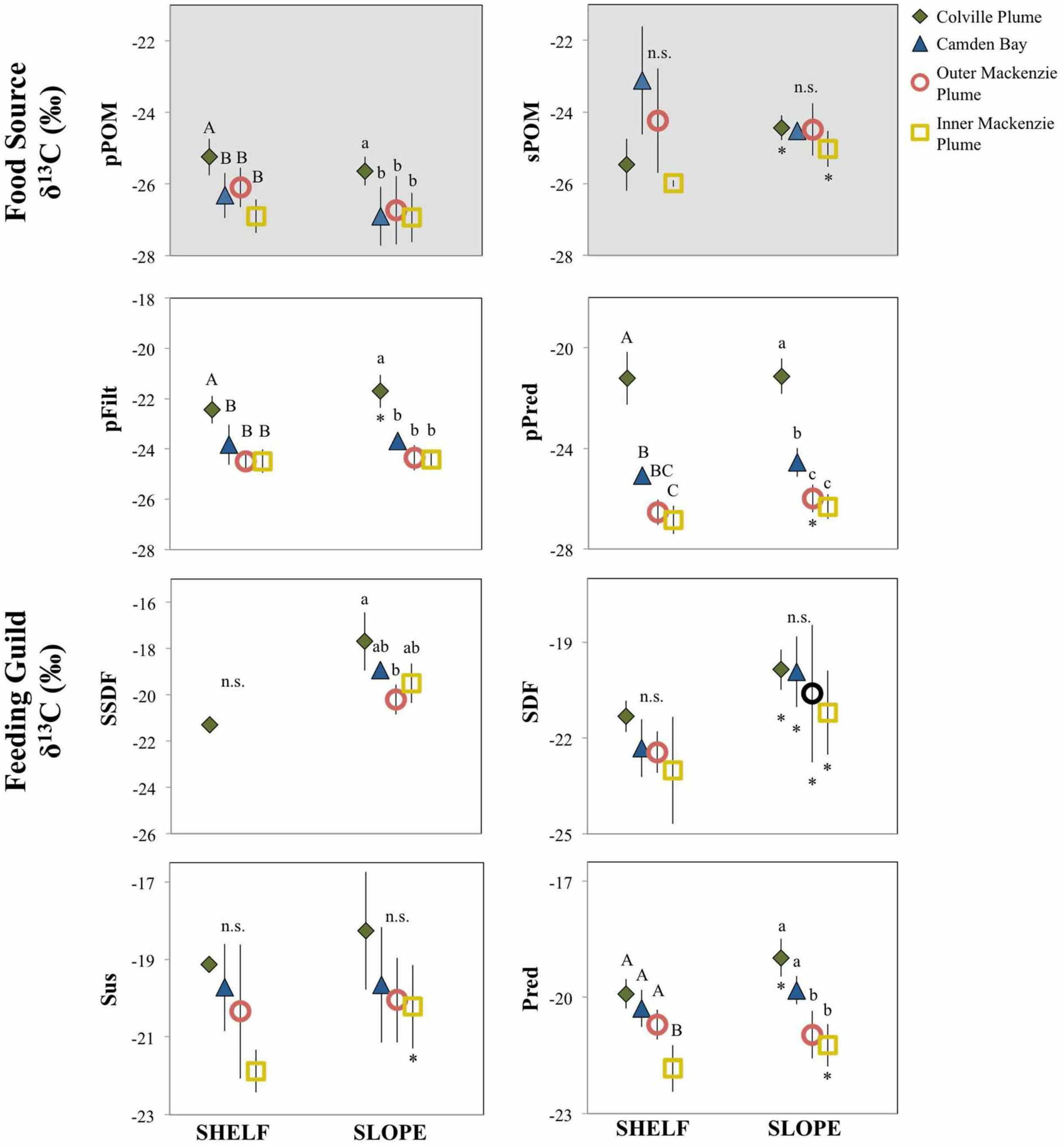

Figure 7. Mean (±SD) $\delta^{13}C$ values (‰) of possible food sources (pPOM and sPOM; shaded background) and consumer feeding guilds (white background), by region and depth group (shelf or slope). Letters denote significantly different groupings among regions, comparing shelf (upper case) and slope (lower case) depth groups separately. Asterisks (*) denote significant differences between shelf versus slope depth groups within the same region. Note that $\delta^{13}C$ scale differs between rows.

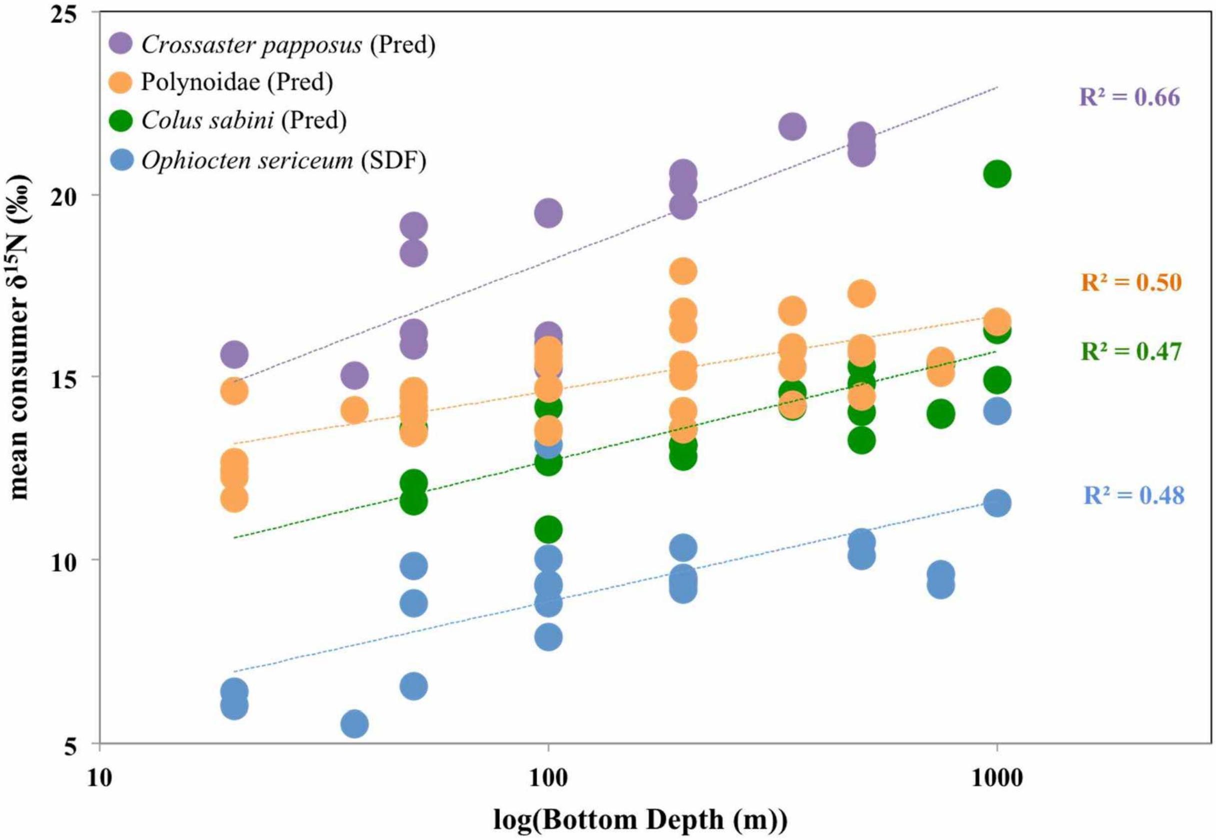

Figure 8. Select benthic consumers' $\delta^{15}N$ values (‰) by bottom depth on log-scale, across all regions. Each point represents the replicate mean $\delta^{15}N$ value of a consumer at one station. All trends significant; linear regression trend lines are shown with respective R^2 values.

6), though statistical power to verify this trend was low due to lack of sediment samples and sample replicates.

Food web length differed slightly among regions and between the shelf and the slope when either pPOM or a primary consumer was used to determine the relative trophic positions of taxa. When pPOM was used as the baseline food source (Fig. 9A), food web lengths based on the highest consumer TP ranged from 4 to 6 TL, and were longer on the slope compared with the shelf in the CP and CB regions. In the OMP region, an apparent difference in food web length on the shelf versus the slope was largely driven by a single predator occupying the highest TP, the sea star *Icasterias panopla*. Food web structure standardized to the δ^{15}N value of primary consumer *Ophiocten sericeum* as TP 2 (Fig. 9B) differed considerably from pPOM-based food webs. CP region shelf and slope food webs based on the primary consumer were 1.1 and 1.3 TL shorter, respectively, than when using pPOM as a baseline. As a result, CP food webs changed from being relatively long compared with all other regions to being relatively short. This change in the CP region occurred because many of the taxa that fell within TL 2 with a pPOM baseline fell within TL 1 when using the primary consumer as a baseline. Though these consumer taxa were also present in the other regions, they occupied higher TPs than the TL 2 represented by the primary consumer *Ophiocten sericeum*. Consequently, the longer food webs in the CB, OMP, and IMP regions were accompanied by an apparent trophic gap between pPOM and the lowest primary consumer, excluding the cumaceans *Diastylis* spp. that had extremely low TP. Food web structure across shelf and slope depth groups were similar to one another in the IMP and OMP regions when using the primary consumer baseline.

The relative distribution of epibenthic consumer biomass by trophic levels using the primary consumer baseline differed among regional food webs (Fig. 10). Within each region, shelf food webs had a much higher proportion of biomass contained in TL 2 than in corresponding slope food webs, regardless of number of species represented per TL. CP region shelf and slope food webs both had a significantly higher proportion of biomass in TLs 1 and 2 than all other regions, with TL 1-2 composing 94% of biomass on the CP shelf and 41% of biomass on the CP slope. In contrast, in CB, OMP, and IMP regions, consumers at TL 3-5 represented the majority of biomass, accounting for 70-79% of biomass in shelf food webs and 91-96% of biomass in slope food webs. Species included in biomass calculations by trophic level accounted for 54% to 88% of the total biomass at each region, which was estimated to be a low of 760 g wet wt * 1000 m^{-2}

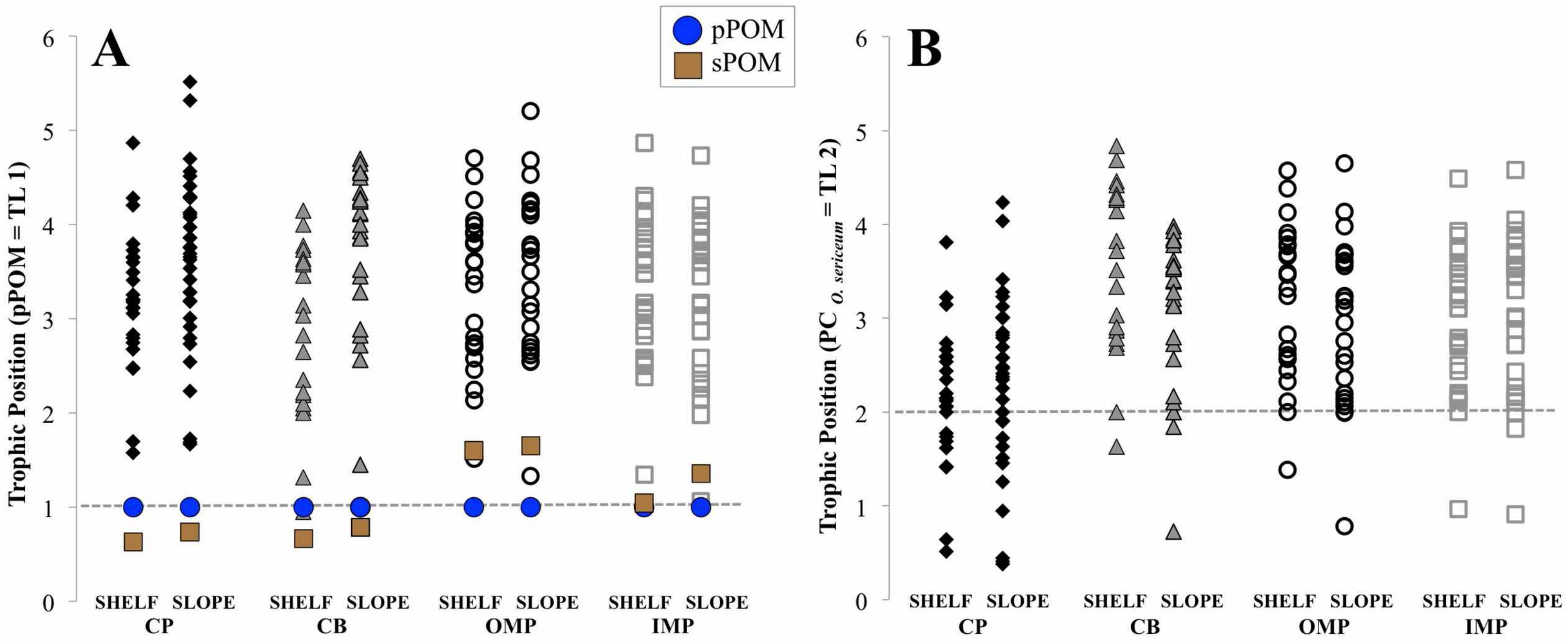

Figure 9. Trophic positions of all consumers by shelf and slope regions. Food webs are based on baselines of pPOM δ^{15}N = TL 1 (**A**) or the primary consumer (PC) *Ophiocten sericeum* δ^{15}N = TL 2 (**B**).

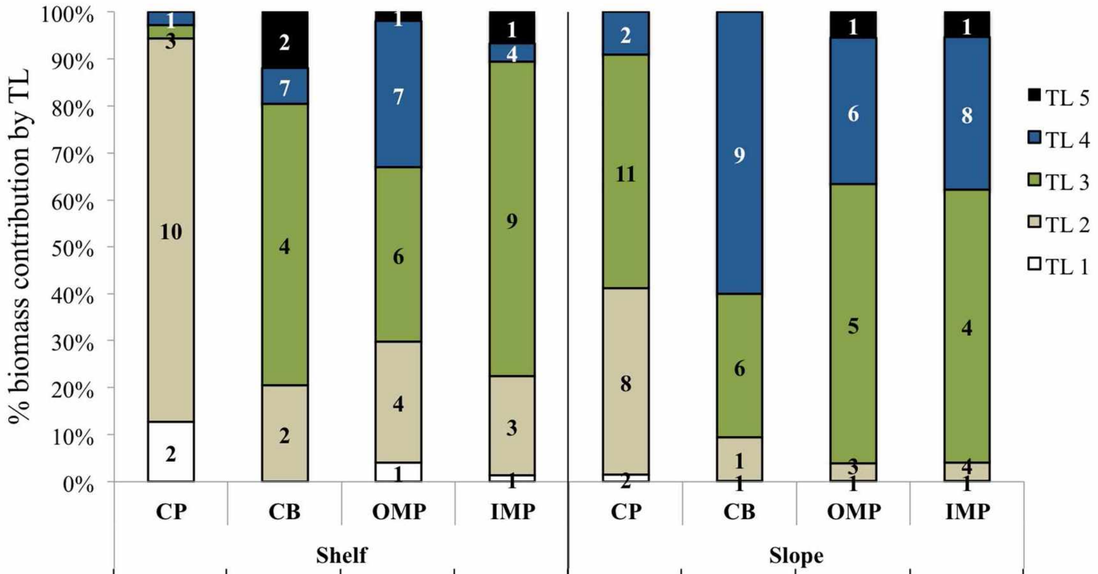

biomass represented	N/A	88%	54%	55%	N/A	81%	68%	61%
Total epifaunal biomass g wet wt * 1000 m^{-2}	773*	6,492	10,712	4,555	118,918*	3,048	3,432	1,832

Figure 10. Relative biomass of consumers within each trophic level based on using a primary consumer baseline (see Fig. 9B), by shelf and slope regions. Histogram labels indicate the number of taxa included in each bar section. Due to some mismatches between available biomass and isotope data from the same stations, these data represent a subset of all taxa included in the food web analyses. Total mean epifauna biomass calculated for each region and percent of total mean biomass represented by taxa in this figure are indicated. CP region total mean biomass estimates (indicated with *) were acquired from data collected during a different project in 2011 (Ravelo et al. in review), separate from this study's sampling effort, and could thus not be directly matched with isotope samples (indicated by N/A). Total biomass for CP slope region only represents data from the upper slope (200 m), and thus is likely an overestimate of actual average CP slope biomass from 200 to 1000 m (see methods).

on the CP shelf to a high of 118,918 g wet wt * 1000 m^{-2} on the CP slope (Fig. 10). It should be noted that the high biomass estimate for the CP slope is based only on data from the upper CP slope (~200 m bottom depth), and thus may overestimate the actual average CP slope biomass across the full 200 to 1000 m depth range, as biomass tends to decrease with greater depth. For example, if biomass estimates for the CB, OMP, and IMP slopes were constrained only to the 200 m stations, they would be 1.5 to 3.1 times higher than estimates containing biomass data from all slope stations to 1000 m. Low percentage biomass representation on the OMP and IMP shelves resulted from insufficient sampling of dominant taxa for stable isotopes at some stations in these locations.

Discussion

Freshwater and terrestrial matter distribution and utilization

In this study, surface water δD values in the upper 5 m (Fig. 3) across the eastern Beaufort Sea suggested Mackenzie Plume influence westward of the Mackenzie Delta. Typically, the Coriolis force directs the Mackenzie Plume to the east of the river delta; however, being at the surface in an Ekman layer, the plume can react rapidly to easterly wind stress, which can drive the Mackenzie-derived waters offshore and to the west (Macdonald and Yu 2006; Mulligan et al. 2010). As would be expected, δD values were lowest nearest the outflow of the river in the IMP region and became higher moving farther offshore over the Beaufort slope. In contrast, in the OMP region, the lowest surface water δD values were at offshore locations, while highest surface water δD values were found nearshore. These trends may be explained by an easterly wind regime: easterly winds recorded over 5 m s^{-1} at Tuktoyaktuk, Northwest Territory, Canada, were sustained for the 48 hrs immediately preceding sampling dates of the OMP and IMP regions (The Weather Underground, Inc.), ideal conditions for upwelling on the Beaufort shelf (Carmack and Kulikov 1998; Williams et al. 2006). Under such conditions, the associated Ekman transport of the Mackenzie surface plume would follow a northerly track offshore nearly parallel to IMP transects, while marine water upwelled over the shelf-break forced by isobath divergence near Herschel Island would reach the surface waters in the nearshore OMP (Macdonald and Yu 2006; Williams et al. 2006; Williams and Carmack 2008). There, Herschel Island acts to divert westward-flowing Mackenzie plume surface water away from the coast, allowing a pocket of upwelled water to remain close to shore (ibid.). The relatively colder and more saline water observed at the surface in the nearshore OMP compared to nearshore surface waters of all other regions supports the presence of upwelling in this region at the time of sampling.

Outside of the IMP, OM_{terr} traced by δD values of surface sediments was not associated with the presence of Mackenzie-River derived freshwater at the time of sampling. The high δD values of all sPOM samples (-170 to -50‰) relative to endmember δD value estimates for both terrestrial (-229‰ ± 19‰) and marine (-183‰ ± 26‰) production indicates that sPOM organic matter had undergone significant biological transformation from its source material(s) (Goñi et al. 2000; Connelly et al. 2012). Assuming that OM_{terr} is indeed characterized by a δD value that is distinct from and lower than that of marine production, and without knowing the δD value changes associated with trophic fractionation, the total range of observed sPOM δD values should only be considered as a relative measure of OM_{terr} influence. If the Mackenzie surface plume were responsible for transporting the majority of OM_{terr} found on the Beaufort shelf and slope (as suggested by Goñi et al. 2013), a gradient of decreasing OM_{terr} away from the point source of the Mackenzie River Delta would be expected in sPOM samples, regardless of the absolute OM_{terr} endmember δD value. Instead, across all shelf regions from the Mackenzie River in the east to the Colville River to the west, sPOM samples spanned a similar range of δD values, with no identifiable spatial gradient of OM_{terr} influence. This finding agrees with past observations of consistently high terrestrial biomarker ratios in sediments across the U.S. Beaufort slope (Naidu et al. 2000; Goñi et al. 2000). Considering that OM_{terr} derived from coastal erosion may have lower, and thus more distinctive δD values than OM_{terr} originating from the Mackenzie River basin (see methods), these data indicate that coastal erosion may be a large contributor of OM_{terr} westward of the Mackenzie River Delta (Goñi et al. 2013).

Benthic invertebrate tissue δD values also showed no correlation with Mackenzie River freshwater distribution at the surface as traced by δD; instead, benthic invertebrate δD values consistently increased in all investigated taxa with depth across all regions. This pattern could be interpreted as decreasing OM_{terr} and increasing marine matter influence with increasing bottom depth, if the relative δD values of benthic consumers were assumed to solely represent relative utilization between terrestrially-derived versus marine-derived food sources. It is possible that these consumers can preferentially assimilate a particular type of organic material when both marine and terrestrial production are present (Martineau et al. 2004; Casper et al. 2014), which could bias their δD values so that they are not a direct reflection of the composition of available organic matter. However, the similar trend observed across several species and feeding types suggests that the increase in consumer tissue δD values with depth is a true reflection of change in the δD values of the bulk organic matter available at the benthos. A regular, depth-related trend across regions with no east to west difference is consistent with a geographically continuous source of OM_{terr} into the Beaufort, such as permafrost soil erosion along the Beaufort coast (Ping et al. 2011; Goñi et al. 2013). OM_{terr} originating from coastal erosion inputs would presumably become increasingly diluted with marine-derived production with distance from shore (Goñi et al. 2013), and thus would feature less prominantly in the tissues of benthic consumers with depth down the Beaufort slope.

A slightly different pattern of OM_{terr} distribution and usage emerged from $\delta^{13}C$ and $\delta^{15}N$ data, however. Those stable isotope values of pPOM and sPOM across the study area indicate a high proportion of OM_{terr} influence over both the Beaufort shelf and slope. The relative low C:N values (< 10 for 82% of POM samples) in this terrestrially-dominated study area are surprising, especially given the higher sPOM C:N values found in prior studies across the Beaufort Sea (Goñi et al. 2000). Since C:N values are known to be more susceptible to biogeochemical alteration than $\delta^{13}C$ values (Thorton and McManus 1994), and considering the high degree of microbial processing associated with both marine and terrestrial matter in the Beaufort Sea (Ortega-Retuerta et al. 2012; Kellogg and Deming 2014; Rontani et al. 2014), $\delta^{13}C$ values were considered to be a more conservative tracer of terrestrial versus marine origins of organic matter in this study. Within regions, the relative proportion of OM_{terr} versus marine organic matter influence in pPOM samples was not significantly different in surface waters moving away from shore (Fig. 6), contrasting with the observed gradients of Mackenzie River plume freshwater in the surface water mass layers of each region (Fig. 3). This finding may indicate that OM_{terr} initially entrained within the Mackenzie surface plume is at some point disassociated from plume dynamics and is advected independently, reaching lateral distances and depths that the plume's water mass does not (Forest et al. 2007, 2013; Goñi et al. 2000). It is also possible that other vectors of OM_{terr} into the Beaufort Sea (e.g., coastal erosion) contributed significantly to the proportion of OM_{terr} present in pPOM and sPOM samples at Beaufort slope stations.

Mixing model analyses may overemphasize contributions of iPOM and marine production to pPOM and sPOM samples. The $\delta^{13}C$ value ascribed to the iPOM endmember was likely at the lower end of the mean seasonal iPOM $\delta^{13}C$ value (see methods; Gradinger et al. 2009), resulting in a possible overestimate of iPOM contributions in mixing models. In addition, no sea ice was encountered during this study's late-summer sampling efforts, and the majority of Arctic ice-associated production is either consumed rapidly within 7-20 days after deposition at the benthos (McMahon et al. 2006; Sun et al. 2007), or else composes only a small fraction of the long-term pool of sediment organic matter (North et al. 2014). Arguably, mixing model analysis constrained to the assumption of negligible isotopic enrichment between organic matter sources and POM samples probably underestimates OM_{terr} inputs and overestimates marine and ice-associated production inputs to pPOM and sPOM. Particle-associated microbial metabolism of OM_{terr} entering the Beaufort from the Mackenzie River is a highly important component of organic matter processing in this region (Parsons et al. 1988, 1989; Vallières et al. 2008; Garneau et al. 2009; Ortega-Retuerta et al. 2012; Rontani et al. 2014). As OM_{terr} gets transformed by microbial break-down, it can result in an increase in $\delta^{13}C$ and $\delta^{15}N$ values (Macko and Estep 1984; Vander Zanden and Rasmussen 2001; Post 2002b), and consequently may become less isotopically distinct from marine production. Thus, pPOM and sPOM data should be interpreted assuming some degree of isotopic transformation accompanying microbial metabolism of POM during its transit to the bottom of the Beaufort shelf and slope (Macko and Estep 1984) as opposed to direct mixing between untransformed organic matter sources. Unfortunately, lacking precise knowledge of the ^{13}C and ^{15}N fractionation factors associated with microbial processing (Lehmann et al. 2002, and references therein), it is difficult to estimate the degree to which this activity may disguise the influence of OM_{terr} via isotope enrichment.

Regardless of mixing model analysis shortcomings, grouping pPOM and sPOM samples by mean $\delta^{13}C$ values of region and depth group (shelf or slope) provided a spatial perspective of relative carbon source differences (Fig. 7). Significant ^{13}C enrichment in pPOM samples at the CP region indicates the relative increase in marine production inputs to the western study area that agrees with recent studies on biotic density patterns in the western Beaufort Sea (Logerwell et al. 2011; Ravelo et al. in review). In contrast, lack of a consistent pattern in the $\delta^{13}C$ values of sPOM across regions on both the shelf and slope may be a result of various distribution and mixing mechanisms of sPOM in this region. Relatively homogenous sPOM $\delta^{13}C$ values may be a consequence of large vertical and horizontal flux (Forest et al. 2013) from upwelling events (Williams et al. 2006), bottom resuspension (Forest et al. 2007), and lateral advection (Hwang et al. 2008). These transport vectors can cause the terrestrial versus marine composition of sPOM to vary irregularly and thus show no consistent trend across the Beaufort shelf (Goñi et al. 2000; Divine et al. in review), even within a dominant pattern of increasing contributions of marine production moving westward from the Mackenzie River outflow (Goñi et al. 2013). Fresh marine production may also be rapidly utilized in the water column by pelagic fauna or by benthic consumers (Bessière et al. 2007; Renaud et al. 2008; Morata et al. 2008) so that little record of its presence remains in marine sediments.

It is valuable to consider the differing trends in pPOM and sPOM $\delta^{13}C$ values in combination to understand which of these two POM sources were being utilized by pelagic and benthic consumers. For example, pelagic consumer isotopic values in the CP region paralleled the higher (marine-derived) pPOM $\delta^{13}C$ values relative to pelagic taxa in all other regions, suggesting direct utilization of marine production and detritus from the water column. Relatively higher marine production in the CP region may derive both from local inputs as well as supplementary inputs of marine production advected into the CP region from the far-western Beaufort and Chukchi seas (Ashjian et al. 2005; Bates et al. 2005; Okkonen et al. 2009). At the benthos, suspension and deposit feeder $\delta^{13}C$ values were not significantly different across most regions, perhaps due to utilization of the more isotopically consistent sPOM food source. Mixing processes within the sediment may have muted the east to west decrease in OM_{terr} inputs for consumers feeding directly on sPOM as discussed above. However, the matching regional $\delta^{13}C$ patterns between benthic predators and pPOM, as well as an obvious trend of ^{13}C enrichment from eastern to western regions on both the shelf and the slope in all feeding guilds (even where non-significant) supports an overall transition in food source from more of the ^{13}C-depleted, OM_{terr} in the east to more of the ^{13}C-enriched, marine production in the west.

Differences between trends in δD and $\delta^{13}C$ values from sPOM and marine consumers contest the applicability of δD values as a tracer of organic matter origins in the Beaufort Sea. $\delta^{13}C$ values of pPOM and biota imply a decreasing influence of terrestrial matter from east to west across both the Beaufort shelf and slope, while δD values suggest that terrestrial matter influence is depth related but independent of proximity to the Mackenzie River outflow. In view of the extensive literature supporting a gradient of increasing OM_{terr} across the Beaufort shelf with proximity to the Mackenzie River (Dunton et al. 1989; Saupe et al. 1989; Schell et al. 1998; Goñi et al. 2000; Naidu et al. 2000), the trend seen in $\delta^{13}C$ values of pPOM and consumer tissues in this study are well-corroborated. It is possible that the distinct water masses layered over the Beaufort shelf and slope (Lansard et al. 2012) drive variation in δD values of marine consumers, as between 30-50% of tissue protein can arise from δD values of ambient H_2O surrounding the animal (Solomon et al. 2009; Soto et al. 2013). The various water masses in which the benthos of the Beaufort shelf and slope resides (Fig. 2) are characterized by δD values ranging from -10‰ in surface waters to +14‰ in Canada Basin deep water (Lansard et al. 2012), generally becoming enriched in deuterium with increasing depth. This 22‰ variation in water mass δD values may therefore contribute to the enrichment of deuterium in consumer tissue with depth in addition to δD contributions from food sources.

δD values of sPOM and consumers may also be affected by isotopic fractionation of organic matter during its transit to depth. Bacterial degradation and remineralization processes are functions of water depth (Robinson et al. 2012), or sinking time of surface organic material (Macko and Estep 1984), resulting in a marked increase in some isotope ratios with depth such as $\delta^{15}N$ values in POM (Altabet and Francois 2001). For $\delta^{15}N$ this increase may be > 10‰ from 0 to 1000 m (Mintenbeck et al. 2007), indicative of increasingly degraded organic matter. Akin to POM $\delta^{15}N$ values, POM δD values may undergo a similar increase during metabolic turnover (e.g., Malej et al. 1993; Birchall et al. 2005), which would imply that POM δD values are also susceptible to isotopic transformation during sinking in the water column. Indeed, both δD and $\delta^{15}N$ values of the same set of benthic consumers increased with increasing bottom depth.

While rough calculations of the δD values of terrestrial plant material and marine phytoplankton (see methods) indicate that these organic matter endmembers could be significantly different, the variability inherent in the meteorological and chemical factors involved in hydrogen isotope discrimination during photosynthesis (Hondula et al. 2014; Yang et al. 2014) speaks to the tenuous nature of these estimates. Moreover, the degree to which δD values are affected by biological fractionation during trophic transfers is not well resolved (Doucett et al. 2007, and references therein). The number of potential variables that could affect the δD values of sPOM and benthic consumers calls into question the interpretation of these data. Given these constraints, $\delta^{13}C$ values are considered the more comprehensive and reliable measure of OM_{terr} influence and consumers' relative utilization of marine versus terrestrial organic matter sources in this analysis.

Trophic structure by depth and terrestrial matter influence

Regional differences in trophic structure corresponded well with trends in the extent of terrestrial organic matter utilization as seen in $\delta^{13}C$ values of consumers. A comparison of food web structure using both pPOM and benthic primary consumer $\delta^{15}N$ ratios as baseline values allowed for an assessment of the connectivity between pelagic and benthic components of each food web. This combined approach is necessary and useful, because this study included both benthic and pelagic taxa, and $\delta^{13}C$ analysis revealed trends in pPOM and pelagic consumer isotope ratios that were not seen in benthic taxa. In the CP region, shorter food web length of PC-based versus pPOM-based food webs indicated that energy flow was tightly coupled among consumers once food sources were utilized at the seafloor, but not well-coupled to pPOM. Given that benthic consumers typically respond rapidly to fresh marine production (Witte et al. 2003; Moodley et al. 2005; Renaud et al. 2008), which pPOM $\delta^{13}C$ values indicate is present in higher proportion in the CP region compared with more eastern Beaufort regions, the trophic decoupling between pPOM and consumers suggests that the pPOM at time of sampling was not representative of long-term consumer food sources. In contrast, little differences in overall food web length between pPOM-based and PC-based food webs in the CB, OMP, and IMP regions implied that energy flow to consumers through the food web in these eastern regions was derived initially from the same organic matter sources reflected in pPOM composition.

The organisms connecting the pPOM food source to mid-level ($TP \geq 2$) benthic consumers in the CB, OMP, and IMP regions were not sampled in this study, leaving a trophic gap between pPOM and pelagic and benthic consumers that was not observed in the western CP region. It is unlikely that unsampled plankton or epifauna taxa occupy this gap, as the majority of taxa that occupied $TP < 2$ in the PC-based food webs of the CP region also occurred in CB, OMP, and IMP food webs, but were displaced to higher trophic positions in these eastern regions. The only sampled taxa consistently within the "trophic gap" were the cumaceans *Diastylis* spp., categorized as surface deposit feeders but whose anomalous trophic positions in multiple food web studies suggest they may fractionate differently or feed on labile food sources not accounted for by these studies (Iken et al. 2005; Bergmann et al. 2009; Renaud et al. 2011). In the CB, OMP, and IMP regions, this trophic gap may be due to recurrent isotopic fractionation caused by microbial break-down of organic matter. Because OM_{terr} is largely composed of complex structural materials from vascular plants such as cellulose and xylan, it can be difficult for marine primary consumers to assimilate directly as they lack the necessary digestive enzymes (Tenore 1983, and references therein). Microbial decomposition of OM_{terr} can effectively break down these complex structures, enabling a higher proportion of the energy available in OM_{terr} to then be utilized as a food source by marine consumers (Tenore 1983; Parsons et al. 1988; Garneau et al. 2009). The presence of a trophic gap in the terrestrially-influenced food webs of this study substantiates the critical role of the microbial loop in connecting OM_{terr} to marine consumers in the eastern Beaufort (Vallières et al. 2008; Garneau et al. 2009; Rontani et al. 2014).

pPOM-based food webs were slightly longer on the slopes of the CP, CB, and OMP regions relative to the respective shelf regions, likely a function of the observed enrichment in consumer

$\delta^{15}N$ values with bottom depth across most taxa. A possible explanation for this pattern is from enrichment of organic matter in ^{15}N with increasing water depth as suggested above (Mintenbeck et al. 2007; Robinson et al. 2012), which is not accounted for when using the near-surface pPOM samples as a food web baseline. Another explanation is that OM_{terr} is depleted in ^{15}N by approximately 6‰ compared with marine-derived matter (Dunton et al. 2006; McTigue and Dunton 2013). Therefore, an increase in organic matter $\delta^{15}N$ values would be anticipated when moving from nearshore regions with greater influence of OM_{terr} to offshore regions with higher inputs of marine production. However, pPOM $\delta^{13}C$ or $\delta^{15}N$ values did not reveal a gradient of decreasing OM_{terr} influence moving away from shore over the Beaufort slope. Furthermore, a substantial increase in $\delta^{13}C$ values of sPOM and consumers with increasing bottom depth would also be expected if relative terrestrial versus marine endmember contributions were primarily responsible for driving these trends in carbon isotope values (e.g., Dunton et al. 2006; Casper et al. 2014), but $\delta^{13}C$ data showed few significant differences between carbon sources to pPOM, sPOM, and consumers on the shelf versus the slope. Even for the limited regions and feeding guilds showing some depth-related enrichment in ^{13}C on the slope relative to the shelf, it is possible that this reflected a small but significant enrichment in ^{13}C with trophic level (Vander Zanden and Rasmussen 2001), as would occur during microbial metabolism during organic matter sinking. Regardless of the cause, the consistent trend of consumer tissue ^{15}N enrichment with depth demonstrates the importance of using a depth-normalized approach to food web analysis (Roy et al. in review) to correct for variables related to station bottom depth, and their effect on stable isotope values.

The likeness of shelf and slope carbon sources and food web structure in the two regions closest to the Mackenzie River (IMP and OMP) speaks to the overwhelming influence of OM_{terr} from this source in the eastern Beaufort Sea. The transport and advection of OM_{terr} from the Mackenzie River down the Beaufort slope (Goñi et al. 2000) may be facilitated by the morphology of the Beaufort Sea's relatively narrow shelf and steep slope compared to shelves of the Eurasian Arctic (Jakobsson et al. 2004), frequent upwelling and resuspension processes (Forest et al. 2013), and vertical convection of brine-enriched waters from sea ice melt (Dittmar 2004). The high mobility of Mackenzie-derived OM_{terr} across the Beaufort and into the Canada Basin has been explored thoroughly in sedimentary markers (Belicka et al. 2002; Forest et al. 2007; Connelly et al. 2012; Goñi et al. 2013), yet consideration of how this OM_{terr} influences the biota of offshore and deep-sea communities in the Arctic Ocean has been inadequate, especially given the potential of terrestrially-derived food subsidies for deep-sea consumers elsewhere (Dittmar 2004; Hunter et al. 2013). The equivalent lengths of shelf and slope food webs in the OMP and IMP regions indicate that the trophic effect of OM_{terr} break-down via the microbial pathway appears to be the same regardless of water depth or the differing benthic community composition (Nephin et al. 2014) between the eastern Beaufort shelf and slope. These findings imply that the microbial communities responsible for processing OM_{terr} at deep locations on the Beaufort slope may have a similar function to the benthic microbial fauna of the sub-Arctic deep-sea, which are the primary assimilators of refractory organic matter sources prior to being consumed by macrofauna (Gontikaki et al. 2011).

In all regions where the food web was characterized by a low trophic level gap (i.e., CB, IMP, OMP), larger proportions of biomass were represented by higher trophic levels across shelf or slope depth groups in comparison to those on the CP shelf or slope (Fig. 10). These regions with high biomass at higher trophic levels were also the regions that received a greater amount of terrestrial production. The inferred presence of the microbial loop at the lower trophic levels of these food webs leads to the occurrence of macro-consumer biomass at a higher TL than it presumably would were microbial processing absent. Apparently, this was the case in the CP region, where the greater inputs of marine production caused shorter food webs fueled with proportionally more biomass at lower trophic levels. Total epifauna biomass, in contrast, did not have a discernable relationship with food web structure. In the shorter food webs of the CP region, total epibenthic biomass on the shelf was several times lower than in the longer, more OM_{terr}-supported shelf food webs of the eastern regions, while biomass on the CP slope was several orders of magnitude higher than on the slope of all other regions. It is possible that the biomass estimates in the CP region are not a good match for the trophic structure calculated for this region, because they were taken from a different study and a narrow depth range. That study does suggest, however, that nutrient-rich water of a Pacific-origin indeed leaves a stronger biomass footprint on the upper slope epifauna of the western Beaufort than on the shelf (Ravelo et al. in review).

Since marine primary productivity in the terrestrially-influenced Beaufort Sea (30-70 g C m^{-2} yr^{-1}) is substantially lower than in other Pacific Arctic seas like the Chukchi (20 to > 400 g C m^{-2} yr^{-1}), which are characterized by high benthic biomass (Sakshaug 2004; Dunton et al. 2005), there must be additional energy subsidies that support higher trophic level consumers in the eastern study regions of the Beaufort Sea. Proportionally higher biomass of taxa at higher trophic levels is presumably sustained by substantial proportions of energy processed through microbial communities and transferred to these consumers at TL 4 and 5. Well-developed microbial communities specifically associated with terrestrial matter in the Beaufort Sea have high efficiency of metabolic OM_{terr} turnover even under low temperature conditions (Vallières et al. 2008; Garneau et al. 2009; Ortega-Retuerta et al. 2012; Rontani et al. 2014). Thus, although the total primary production available to marine consumers in the highly OM_{terr}-influenced eastern Beaufort Sea is lower than in the western regions of the Pacific Arctic (Sakshaug 2004), microbial activity processing OM_{terr} may enable the efficient use of available food sources.

The results presented here refute the theory that OM_{terr} is unusable or a poor food source for marine consumers (e.g., Schell 1983; Thorp and Delong 2002; Berglund et al. 2007). Though understanding of the biochemical effects of microbial metabolism on OM_{terr} remains poor, zooplankton biomass, fish growth, and total food web efficiency can be positively correlated with terrestrially-associated microbial production when temperature is simultaneously increased (Lefébure et al. 2013). In view of the significant warming at high latitudes projected to co-occur with increases of terrestrial matter inputs to the Arctic Ocean (ACIA 2004; Lantuit et al. 2012; Holmes et al. 2013), climate change may provide a suitable environmental setting for heightened OM_{terr}-associated microbial productivity in Arctic regions such as the Beaufort Sea. Combined with the conclusion in this study that microbial processes may fill a critical trophic gap in terrestrially-influence food webs, these results suggest that the microbial metabolism may enhance the quality of OM_{terr} (e.g., Decho 1990; Klein Breteler et al. 1999), transforming it into a valuable and efficient food source for marine consumers in the eastern Beaufort Sea.

Conclusion

The interplay of high inputs of terrestrial organic matter (OM_{terr}) into the Beaufort Sea from Canada's Mackenzie River with advected and *in situ* marine primary production drives variation in marine trophic structure across the Beaufort shelf and slope. Stable isotope analyses of surface water, particulate organic matter, and pelagic and benthic consumers from locations ranging from 20 to 1000 m bottom depth revealed a strong isotopic imprint of OM_{terr} in the eastern Beaufort Sea, which decreased moving westward from the Mackenzie River. Concurrent with high OM_{terr} influence, shelf and slope food webs in the eastern Beaufort Sea were characterized by the inferred presence of strong microbial processing, which increased food web length and resulted in a greater proportion of epibenthic macro-consumer biomass at higher trophic levels compared to western Beaufort Sea food webs. In view of major differences in quantitative primary production available to marine consumers across the Beaufort Sea, this study has provided evidence that the energetic value and transfer efficiency of OM_{terr} through marine food webs is higher than previously thought.

Terrestrially-derived energetic support for Arctic marine consumers likely has significant consequences for marine communities in the face of increased river runoff and coastal erosion inputs into the Arctic Ocean (Lantuit et al. 2012; Holmes et al. 2013). An adaptive microbial loop that expands its activity and production in response to increased OM_{terr} contributions in the Beaufort Sea (as suggested by Ortega-Retuerta et al. 2012) would not only facilitate regeneration of dissolved terrestrially-derived nutrients to be utilized in marine primary production (Tank et al. 2012), but could also enable an efficient pathway for OM_{terr} to function as a food source for marine consumers (Lefébure et al. 2013). Given the dynamic and synergistic effects of climate change already being observed in the Arctic (ACIA 2004; Walsh 2008; Wassmann et al. 2011), our ability to make informed predictions of the impacts of shifting organic matter sources in the Beaufort Sea is critical. High-latitude research specifically considering the association between terrestrial matter and the marine microbial loop will be vital in the race to anticipate and mitigate the effects of global change on the biological health of Arctic marine food webs.

References

Abrams PA, Roth JD (1994) The effects of enrichment of three-species food chains with nonlinear functional responses. Ecology 75(4):1118-1130

ACIA (Arctic Climate Impact Assessment) (2004) In: Hassol SJ (ed.) Impacts of a Warming Arctic: Arctic Climate Impact Assessment. Cambridge: Cambridge University Press.

Aitken AE, Fournier J (1993) Macrobenthos communities of Cambridge, Mcbeth and Itirbilung Fiords, Baffin Island, Northwest Territories, Canada. Arctic 46(1):60-71

Altabet MA, Francois R (2001) Nitrogen isotope biogeochemistry of the Antarctic Polar Frontal Zone at 170°W. Deep-Sea Res Pt II 48(19-20):4247-4273

Arim M, Marquet PA, Jaksic FM (2007) On the relationship between productivity and food chain length at different ecological levels. Am Nat 169(1):62-72

Ashjian CJ, Gallager SM, Plourde S (2005) Transport of plankton and particles between the Chukchi and Beaufort Seas during summer 2002, described using a Video Plankton Recorder. Deep Sea Res Pt II 52:3259-3280

Auel H, Werner I (2003) Feeding, respiration and life history of the hyperiid amphipod *Themisto libellula* in the Arctic marginal ice zone of the Greenland Sea. J Exp Mar Biol Ecol 296(2):183-197

Bates NR, Best MHP, Hansell DA (2005) Spatio-temporal distribution of dissolved inorganic carbon and net community production in the Chukchi and Beaufort Seas. Deep Sea Res Pt II 52:3303-3323

Belicka LL, Macdonald RW, Harvey HR (2002) Sources and transport of organic carbon to shelf, slope, and basin surface sediments of the Arctic Ocean. Deep Sea Res Pt I 49(8):1463-1483

Berglund J, Müren U, Båmstedt U, Andersson A (2007) Efficiency of a phytoplankton-based and a bacteria-based food web in a pelagic marine system. Limnol Oceanogr 52(1):121-131

Bergmann M, Dannheim J, Bauerfeind E, Klages M (2009) Trophic relationships along a bathymetric gradient at the deep-sea observatory HAUSGARTEN. Deep-Sea Res I 56:408-424

Bessière A, Nozais C, Brugel S, Demers S, Desrosiers G (2007) Metazoan meiofauna dynamics and pelagic-benthic coupling in the Southeastern Beaufort Sea, Arctic Ocean. Polar Biol 30:1123-1135

Birchall J, O'Connell TC, Heaton THE, Hedges REM (2005) Hydrogen isotope ratios in animal body protein reflect trophic level. J Anim Ecol 74(5):877-881

Bluhm BA, Gradinger R (2008) Regional variability in food availability for Arctic marine mammals. Ecol Appl 18(2):S77-S96

Brown KA, McLaughlin F, Tortell PD, Varela DE, Yamamoto-Kawai M, Hunt B, Francois R (2014) Determination of particulate organic carbon sources to the surface mixed layer of the Canada Basin, Arctic Ocean. J Geophys Res: Oceans 119:1084-1102

Carmack EC, Kulikov EA (1998) Wind-forced upwelling and internal Kelvin wave generation in Mackenzie Canyon, Beaufort Sea. J Geophys Res: Oceans 103(C9):18447-18458

Carmack EC, Macdonald RW (2002) Oceanography of the Canadian Shelf of the Beaufort Sea: a setting for marine life. Arctic 55:29-45

Carmack E, Wassmann P (2006) Food webs and physical-biological coupling on pan-Arctic shelves: unifying concepts and comprehensive perspectives. Prog Oceanogr 71:446-477

Casper AF, Rautio M, Martineau C, Vincent WF (2014) Variation and assimilation of Arctic riverine seston in the pelagic food web of the Mackenzie River Delta and Beaufort Sea transition zone. Estuar Coast doi:10.1007/s12237-014-9917-z

Cividanes S, Incera M, López J (2002) Temporal variability in the biochemical composition of sedimentary organic matter in an intertidal flat of the Galician coast (NW Spain). Oceanol Acta 25:1-12

Connelly TL, Deibel D, Parrish CC (2012) Biogeochemistry of near-bottom suspended particulate matter of the Beaufort Sea shelf (Arctic Ocean): C, N, P, $\delta^{13}C$ and fatty acids. Cont Shelf Res 43:120-132

Cooper LW, Benner R, McClelland JW, Peterson BJ, Holmes RM, Raymond PA, Hansell DA, Grebmeier JM, Codispoti LA (2005) Linkages among runoff, dissolved organic carbon, and the stable oxygen isotope composition of seawater and other water mass indicators in the Arctic Ocean. J Geophys Res 110:G02013

Cooper LW, McClelland JW, Holmes RM, Raymond PA, Gibson J, Guay CK, Peterson BJ (2008) Flow-weighted values of runoff tracers ($\delta^{18}O$, DOC, Ba, alkalinity) from the six largest Arctic rivers. Geophys Res Lett 35:L18606

Craig H (1961) Isotopic variations in meteoric waters. Science 133(3465):1702-1703

Crawford RE, Vagle S, Carmack EC (2012) Water mass and bathymetric characteristics of polar cod habitat along the continental shelf and slope of the Beaufort. Polar Biol 35:179-190

Decho AW (1990) Microbial exopolymer secretions in ocean environments: their role(s) in food webs and marine processes. Oceanogr Mar Biol Annu Rev 28:73-153.

Dittmar T (2004) Evidence for terrigenous dissolved organic nitrogen in the Arctic deep sea. Limnol Oceanogr 49(1):148-156

Divine LM, Iken K, Bluhm BA (in review) Regional benthic food web structure on the Alaskan Beaufort Sea shelf. Mar Ecol Prog Ser.

Doucett RR, Marks JC, Blinn DW, Caron M, Hungate BA (2007) Measuring terrestrial subsidies to aquatic food webs using stable isotopes of hydrogen. Ecology 88(6):1587-1592

Dunton KH, Saupe SM, Golikov AN, Schell DM, Schonberg SV (1989) Trophic relationships and isotope gradients among Arctic marine fauna. Mar Ecol Prog Ser 56:89-97

Dunton KH, Goodall JL, Schonberg SV, Grebmeier JM, Maidment DR (2005) Multi-decadal synthesis of benthic–pelagic coupling in the western Arctic: role of cross-shelf advective processes. Deep-Sea Res Pt II 52(24-26):3462-3477

Dunton KH, Weingartner T, Carmack EC (2006) The nearshore western Beaufort Sea ecosystem: circulation and importance of terrestrial carbon in Arctic coastal food webs. Prog Oceanogr 71(2-4):362-378

Dunton KH, Schonberg SV, Cooper LW (2012) Food web structure of the Alaskan nearshore shelf and estuarine lagoons of the Beaufort Sea. Estuar Coast 35(2):416-435

Feder HM, Iken K, Blanchard AL, Jewett SC, Schonberg S (2011) Benthic food web structure in the southeastern Chukchi Sea: an assessment using $\delta^{13}C$ and $\delta^{15}N$ analyses. Polar Biol 34:521-532

Finlay JC, Doucett RR, McNeely C (2010) Tracing energy flow in stream food webs using stable isotopes of hydrogen. Freshwater Biol 55(5):941-951

Ford JD, Smit B (2004) A framework for assessing the vulnerability of communities in the Canadian Arctic to risks associated with climate change. Arctic 57(4):389-400

Forest A, Sampei M, Hattori H, Makabe R, Sasaki H, Fukuchi M, Wassmann P, Fortier L (2007) Particulate organic carbon fluxes on the slope of the Mackenzie Shelf (Beaufort Sea): physical and biological forcing of shelf-basin exchanges. Journal of Marine Systems 68(1-2):39-54

Forest A, Babin M, Stemmann L, Picheral M, Sampei M, Fortier L, Gratton Y, Bélanger S, Devred E, Sahlin J (2013) Ecosystem function and particle flux dynamics across the Mackenzie Shelf (Beaufort Sea, Arctic Ocean): an integrative analysis of spatial variability and biophysical forcings. Biogeosciences 10(5):2833-2866

Frey KE, Maslanik JA, Kinney JC, Maslowski W (2014) Recent variability in sea ice cover, age, and thickness in the Pacific Arctic region. In: Grebmeier JM, Maslowski W (eds.) The Pacific Arctic region: ecosystem status and trends in a rapidly changing environment, pp. 31-63, Springer:Netherlands

Gajewski K, Viau A, Sawada M, Atkinson D, Wilson S (2001) *Sphagnum* peatland distribution in North America and Eurasia during the past 21,000 years. Global Biogeochem Cy 15(2):297-310

Garneau M-È, Vincent WF, Terrado R, Lovejoy C (2009) Importance of particle-associated bacterial heterotrophy in a coastal Arctic ecosystem. J Marine Syst 75(1–2):185-197

Goñi MA, Yunker MB, Macdonald RW, Eglinton TI (2000) Distribution and sources of organic biomarkers in Arctic sediments from the Mackenzie River and Beaufort Shelf. Mar Chem 71:23-51

Goñi MA, Yunker MB, Macdonald RW, Eglinton TI (2005) The supply and preservation of ancient and modern components of organic carbon in the Canadian Beaufort Shelf of the Arctic Ocean. Mar Chem 93:53-73

Goñi MA, O'Connor AE, Kuzyk ZZ, Yunker MB, Gobeil C, Macdonald RW (2013) Distribution and sources of organic matter in surface marine sediments across the North American Arctic margin. J Geophys Res: Oceans 118(9):4017-4035

Gontikaki E, van Oevelen D, Soetaert K, Witte U (2011) Food web flows through a sub-arctic deep-sea benthic community. Prog Oceanogr 91:245-259

Gradinger R (2009) Sea-ice algae: major contributors to primary production and algal biomass in the Chukchi and Beaufort Seas during May/June 2002. Deep Sea Res Pt II 56:1201-1212

Gradinger R, Kaufman MR, Bluhm BA (2009) Pivotal role of sea ice sediments in the seasonal development of near-shore Arctic fast ice biota. Mar Ecol Prog Ser 394:49-63

Graeve M, Kattner G, Piepenburg D (1997) Lipids in Arctic benthos: does the fatty acid and alcohol composition reflect feeding and trophic interactions? Polar Biol 18(1):53-61

Haahtela I (1990) What do Baltic studies tell us about the isopod *Saduria entomon* (L.)? Ann Zool Fennici 27:269-278

Hall SJ, Raffaelli D (1991) Food-web patterns: Lessons from a species-rich web. J Anim Ecol 60(3):823-841

Hansen JH, Hedeholm RB, Sünksen K, Christensen JT, Grønkjær P (2012) Spatial variability of carbon ($\delta^{13}C$) and nitrogen ($\delta^{15}N$) stable isotope ratios in an Arctic marine food web. Mar Ecol Prog Ser 467:47-59

Hitchon B, Krouse HR (1972) Hydrogeochemistry of the surface waters of the Mackenzie River drainage basin, Canada – III. Stable isotopes of oxygen, carbon, and sulphur. Geochim Cosmochim Ac 36:1337-1357

Hobson KA, Welch HE (1992) Determination of trophic relationships within a high Arctic marine food web using $\delta^{13}C$ and $\delta^{15}C$ analysis. Mar Ecol Prog Ser 84:9-18

Hobson KA, Ambrose WB Jr, Renaud PE (1995) Sources of primary production, benthic-pelagic coupling, and trophic relationships within the Northeast Water Polynya: insights from $\delta^{13}C$ and $\delta^{15}N$ analysis. Mar Ecol Prog Ser 128:1-10

Hobson KA, Fisk A, Karnovsky N, Holst M, Gagnon J-M, Fortier M (2002) A stable isotope ($\delta^{13}C$, $\delta^{15}N$) model for the North Water food web: implications for evaluating trophodynamics and the flow of energy and contaminants. Deep-Sea Res Pt II 49(22–23):5131-5150

Holmes RM, Coe MT, Fiske GJ, Gurtovaya T, McClelland JW, Shiklomanov AI, Spencer RGM, Tank SE, Zhulidov AV (2013) Climate change impacts on the hydrology and biogeochemistry of Arctic rivers. In: Goldman CR, Kumagai M, Robarts RD (eds.) Climatic change and global warming of inland waters: impacts and mitigation for ecosystems and societies. John Wiley & Sons, Ltd: Oxford, UK, pp 3-26

Hondula KL, Pace ML, Cole JJ, Batt RD (2014) Hydrogen isotope discrimination in aquatic primary producers: implications for aquatic food web studies. Aquat Sci 76:217-229

Hunter WR, Jamieson A, Huvenne VAI, Witte U (2013) Sediment community responses to marine vs. terrigenous organic matter in a submarine canyon. Biogeosciences 10:67-80

Hwang J, Eglinton TI, Krishfield RA, Manganini SJ, Honjo S (2008) Lateral organic carbon supply to the deep Canada Basin. Geophys Res Lett 35:L11607

Hwang J, Druffel ERM, Eglinton TI (2010) Widespread influence of resuspended sediments on oceanic particulate organic carbon: insights from radiocarbon and aluminum contents in sinking particles. Global Biogeochem Cy 24:GB4016

Iken K, Brey T, Wand U, Voigt J, Junghans P (2001) Food web structure of the benthic community at the Porcupine Abyssal Plain (NE Atlantic): a stable isotope analysis. Prog Oceanogr 50:383-405

Iken K, Bluhm BA, Gradinger R (2005) Food web structure in the high Arctic Canada Basin: evidence from $\delta^{13}C$ and $\delta^{15}N$ analysis. Polar Biol 28(3):238-249

Iken K, Bluhm B, Dunton K (2010) Benthic food-web structure under differing water mass properties in the southern Chukchi Sea. Deep-Sea Res Pt II 57(1-2):71-85

Jakobsson M, Grantz A, Kristoffersen Y, Macnab R (2004) Bathymetry and physiography of the Arctic Ocean and its constituent seas. In: Stein R, Macdonald RW (eds.) The organic carbon cycle in the Arctic Ocean. Springer:Heidelberg, pp 1–6

Jangoux M, Lawrence JM (1982) Echinoderm nutrition, Rotterdam:CRC Press, 700 p.

Kellogg CTE, Deming JW (2014) Particle-associated extracellular enzyme activity and bacterial community composition across the Canadian Arctic Ocean. FEMS Microbiol Ecol 89(2):360-375

Klein Breteler WCM, Schogt N, Baas M, Schouten S, Kraay GW (1999) Trophic upgrading of food quality by protozoans enhancing copepod growth: role of essential lipids. Mar Biol 135:191-198

Krouse HR, Mackay JR (1971) Application of $H_2{}^{18}O/H_2{}^{16}O$ abundances to the problem of lateral mixing in the Liard–Mackenzie river system. Can J Earth Sci 8(9):1107-1109

Kulikov E, Carmack E, Macdonald R (1998) Flow variability at the continental shelf break of the Mackenzie Shelf in the Beaufort Sea. J Geophys Res: Oceans (1978–2012) 103(C6):12725-12741

Lansard B, Mucci A, Miller LA, Macdonald RW, Gratton Y (2012) Seasonal variability of water mass distribution in the southeastern Beaufort Sea determined by total alkalinity and $\delta^{18}O$. J Geophys Res: Oceans (1978–2012) 117:C03003

Lantuit H, Overduin PP, Couture N, Wetterich S, Aré F, Atkinson D, Brown J, Cherkashov G, Drozdov D, Forbes DL, Graves-Gaylord A, Grigoriev M, Hubberten H-W, Jordan J, Jorgenson T, Ødegård RS, Ogorodov S, Pollard WH, Rachold V, Sedenko S, Solomon S, Steenhuisen F, Streletskaya I, Vasiliev A (2012) The Arctic coastal dynamics database: a new classification scheme and statistics on Arctic permafrost coastlines. Estuar Coast 35(2):383-400

Lefébure R, Degerman R, Andersson A, Larsson S, Eriksson L-O, Båmstedt U, Byström P (2013) Impacts of elevated terrestrial nutrient loads and temperature on pelagic food-web efficiency and fish production. Glob Change Biol 19(5):1358-1372.

Lehmann MF, Bernasconi SM, Barbieri A, McKenzie JA (2002) Preservation of organic matter and alteration of its carbon and nitrogen isotope composition during simulated and in situ early sedimentary diagenesis. Geochim Cosmochim Ac 66(20):3573-3584

Logan JM, Jardine TD, Miller TJ, Bunn SE, Cunjak RA, Lutcavage ME (2008) Lipid corrections in carbon and nitrogen stable isotope analyses: comparison of chemical extraction and modelling methods. J Anim Ecol 77(4):838-846

Logerwell E, Rand K, Weingartner TJ (2011) Oceanographic characteristics of the habitiat of benthic fish and invertebrates in the Beaufort Sea. Polar Biol 34:1783-1796

Lowry LF, Sheffield G, George JC (2004) Bowhead whale feeding in the Alaska Beaufort Sea, based on stomach contents analyses. J Cetacean Res Manage 6(3):215-223

Lundsten L, Paull CK, Schlining KL, McGann M, Ussler W III (2010) Biological characterization of a whale-fall near Vancouver Island, British Columbia, Canada. Deep-Sea Res Pt I 57(7):918-922

Macdonald RW, Carmack EC, McLaughlin FA, Iseki K, Macdonald DM, O'Brien MC (1989) Composition and modification of water masses in the Mackenzie Shelf estuary. J Geophys Res 94(C12):18057-18070

Macdonald RW, Paton DW, Carmack EC, Omstedt A (1995) The freshwater budget and under-ice spreading of Mackenzie River Water in the Canadian Beaufort Sea based on salinity and $^{18}O/^{16}O$ measurements in water and ice. J Geophys Res: Oceans 100(C1):895-919

Macdonald RW, Solomon SM, Cranston RE, Welch HE, Yunker MB, Gobeil C (1998) A sediment and organic carbon budget for the Canadian Beaufort Shelf. Mar Geol 144:255-273

Macdonald RW, Falkner KK, Swift JH (1999) Connections among ice, runoff and atmospheric forcing in the Beaufort Gyre. Geophys Res Lett 26(15):2223-2226.

Macdonald RW, McLaughlin FA, Carmack EC (2002) Fresh water and its sources during the SHEBA drift in the Canada Basin of the Arctic Ocean. Deep-Sea Res Pt I 49(10):1769-1785

Macdonald RW, Naidu AS, Yunker MB, Gobeil C (2004) The Beaufort Sea: distribution, sources, fluxes, and burial rates of organic carbon. In: Stein R, Macdonald RW (eds.) The organic carbon cycle in the Arctic Ocean. Springer:Heidelberg, pp. 177-192

Macdonald RW, Yu Y (2006) The Mackenzie estuary of the Arctic Ocean. Hdb Env Chem 5:91-120

Macdonald TA, Burd BJ, Macdonald VI, van Roodselaar A (2010) Taxonomic and feeding guild classification for the marine benthic macroinvertebrates of the Strait of Georgia, British Columbia. Can Tech Rep Fish Aquat Sci 2874:iv + 63 p.

Macko SA, Estep MLF (1984) Microbial alteration of stable nitrogen and carbon isotopic compositions of organic matter. Org Geochem 6:787–790

Mah CL (2014). *Icasterias panopla* (Stuxberg, 1878). In: Mah CL (2014) World Asteroidea database. Accessed through: Mah, C.L. (2014) World Asteroidea database at http://www.marinespecies.org/asteroidea/aphia.php?p=taxdetails&id=123796 on 2014-11-14

Malej A, Faganeli J, Pezdič J (1993) Stable isotope and biochemical fractionation in the marine pelagic food chain: the jellyfish *Pelagia noctiluca* and net zooplankton. Mar Biol 116(4):565-570

Martineau C, Vincent WF, Frenette J-J, Dodson JJ (2004) Primary consumers and particulate organic matter: isotopic evidence of strong selectivity in the estuarine transition zone. Limnol Oceanogr 49(5):1679-1686

Mauchline J (1998) The biology of calanoid copepods. Academic Press: San Diego, CA

McClelland JW, Holmes RM, Dunton KH, Macdonald RW (2012) The Arctic Ocean estuary. Estuar Coast 35:353-368

McClelland JW, Townsend-Small A, Holmes RM, Pan F, Stieglitz M, Khosh M, Peterson BJ (2014) River export of nutrients and organic matter from the North Slope of Alaska to the Beaufort Sea. Water Resour Res 50:1823-1839

McMahon KW, Ambrose WG Jr, Johnson BJ, Sun M-Y, Lopez GR, Clough LM, Carroll ML (2006) Benthic community response to ice algae and phytoplankton in Ny Ålesund, Svalbard. Mar Ecol Prog Ser 310:1-14

McTigue ND, Dunton KH (2013) Trophodynamics and organic matter assimilation pathways in the northeast Chukchi Sea, Alaska. Deep-Sea Res Pt II 102:84-96

Mecklenburg CW, Mecklenburg TA, Thorsteinson LK (2002) Fishes of Alaska, American Fisheries Society: Bethesda, 1037 p.

Mercier A, Schofield M, Hamel J-F (2011) Evidence of dietary feedback in a facultative association between deep-sea gastropods and sea anemones. J Exp Mar Biol Ecol 396(2):207-215

Meyers PA (1997) Organic geochemical proxies of paleoceanographic, paleolimnologic, and paleoclimatic processes. Org Geochem 27(5/6):213-250

Michener R, Lajtha K, eds. (2007) Stable isotopes in ecology and environmental science. Blackwell Publishing: Oxford, 565 p.

Mintenbeck K, Jacob U, Knust R, Arntz WE, Brey T (2007) Depth-dependence in stable isotope ratio δ^{15}N of benthic POM consumers: the role of particle dynamics and organism trophic guild. Deep-Sea Res Pt I 54(6):1015-1023

Mintenbeck K, Brey T, Jacob U, Knust R, Struck U (2008) How to account for the lipid effect on carbon stable-isotope ratio (δ^{13}C): sample treatment effects and model bias. J Fish Biol 72(4):815-830

Moodley L, Middelburg JJ, Soetaert K, Boschker HTS, Herman PMJ, Heip CHR (2005) Similar rapid response to phytodetritus deposition in shallow and deep-sea sediments. J Mar Res 63:457-469

Morata N, Renaud PE, Brugel S, Hobson KA, Johnson BJ (2008) Spatial and seasonal variations in the pelagic-benthic coupling of the southeastern Beaufort Sea revealed by sedimentary biomarkers. Mar Ecol Prog Ser 371:47-63

Mulligan RP, Perrie W, Solomon S (2010) Dynamics of the Mackenzie River plume on the inner Beaufort shelf during an open water period in summer. Estuar Coast Shelf Sci 89:214-220

Münchow A, Carmack EC (1997) Synoptic flow and density observations near an Arctic shelf break. J Phys Oceanogr 27(7):1402-1419

Naidu AS, Scalan RS, Feder HM, Goering JJ, Hameedi MJ, Parker PL, Behrens EW, Caughey ME, Jewett SC (1993) Stable organic carbon isotopes in sediments of the north Bering-south Chukchi seas, Alaskan-Soviet Arctic Shelf. Cont Shelf Res 13(5/6):669-691

Naidu AS, Cooper LW, Finney BP, Macdonald RW, Alexander C, Semiletov IP (2000) Organic carbon isotope ratios ($\delta^{13}C$) of Arctic Amerasian Continental shelf sediments. Int J Earth Sci 89:522-532

Nephin J, Juniper SK, Archambault P (2014) Diversity, abundance and community structure of benthic macro- and megafauna on the Beaufort shelf and slope. PLoS ONE 9(7):e101556

North CA, Lovvorn JR, Kolts JM, Brooks ML, Cooper LW, Grebmeier JM (2014) Deposit-feeder diets in the Bering Sea: potential effects of climatic loss of sea ice-related microalgal blooms. Ecol Appl 24(6):1525-1542

Okkonen SR, Ashjian CJ, Campbell RG, Maslowski W, Clement-Kinney JL, Potter R. (2009) Intrustion of warm Bering/Chukchi waters onto the shelf in the western Beaufort Sea. J Geophys Res: Oceans 114:C00A11

O'Neil, JR (1968) Hydrogen and oxygen isotope fractionation between ice and water. J Phys Chem 72(10):3683-3684

Ortega-Retuerta E, Jeffrey W, Babin M, Bélanger S, Benner R, Marie D, Matsuoka A, Raimbault P, Joux F (2012) Carbon fluxes in the Canadian Arctic: patterns and drivers of bacterial abundance, production and respiration on the Beaufort Sea margin. Biogeosciences Discuss 9(5):6015-6050

Parnell AC, Inger R, Bearhop S, Jackson AL (2010) Source partitioning using stable isotopes: coping with too much variation. PLoS ONE 5(3):e9672

Parsons TR, Webb DG, Dovey H, Haigh R, Lawrence M, Hopky GE (1988) Production studies in the Mackenzie River – Beaufort Sea Estuary. Polar Biol 8:235-239

Parsons TR, Webb DG, Rokeby BE, Lawrence M, Hopky GE, Chiperzak DB (1989) Autotrophic and heterotrophic production in the Mackenzie River/Beaufort Sea estuary. Polar Biol 9:261-266

Pickart RS (2004) Shelfbreak circulation in the Alaskan Beaufort Sea: mean structure and variability. J Geophys Res 109:C04024

Pickart RS, Spall MA, Mathis JT (2013) Dynamics of upwelling in the Alaskan Beaufort Sea and associated shelf-basin fluxes. Deep-Sea Res Pt 1 76:35-51

Pieńkowski AJ, England JH, Furze MF, MacLean B, Blasco S (2014) The late Quaternary environmental evolution of marine Arctic Canada: Barrow Strait to Lancaster Sound. Quaternary Sci Rev 91:184-203

Piepenburg D (2000) Arctic brittle stars (Echinodermata: Ophiuroidea). Oceanogr Mar Biol Ann Rev 38:189-256

Ping C-L, Michaelson GJ, Guo L, Jorgenson MT, Kanevskiy M, Shur Y, Dou F, Liang J (2011) Soil carbon and material fluxes across the eroding Alaska Beaufort Sea coastline. J Geophys Res: Biogeo 116:G02004

Pomeroy LR, Deibel D (1986) Temperature regulation of bacterial activity during the spring bloom in Newfoundland coastal waters. Science 233(4761):359-361

Pomeroy LR, Wiebe WJ (1988) Energetics of microbial food webs. Hydrobiologia 159:7-18

Post DM (2002a) The long and short of food-chain length. Trends Ecol Evol 17(8):269-277

Post DM (2002b) Using stable isotopes to estimate trophic position: models, methods and assumptions. Ecology 83(3):703-718

R Development Core Team (2014) R: A language and environment for statistical computing. R Foundation for Statistical Computing, Vienna, Austria. Retrieved from <http://www.R-project.org/>

Rachold V, Grigoriev MN, Are FE, Solomon S, Reimnitz E, Kassens H, Antonow M (2000) Coastal erosion vs riverine sediment discharge in the Arctic Shelf seas. Int J Earth Sciences 89:450-460

Rachold V, Eicken H, Gordeev VV, Grigoriev MN, Hubberten H-W, Lisitzin AP, Shevchenko VP, Schirrmeister L (2004) Modern terrigenous organic carbon input to the Arctic Ocean. In: Stein R, Macdonald RW (eds.) The organic carbon cycle in the Arctic Ocean. Springer:Heidelberg, pp. 33-55

Ravelo AM, Konar B, Bluhm BA (in review) Spatial variability of epibenthic communities on the Alaska Beaufort Sea shelf. Polar Biol

Renaud PE, Morata N, Carroll ML, Denisenko SG, Reigstad M (2008) Pelagic-benthic coupling in the western Barents Sea: processes and time scales. Deep Sea Res Pt II 55:2372-2380

Renaud PE, Tessmann M, Evenset A, Christensen GN (2011) Benthic food-web structure of an Arctic fjord (Kongsfjorden, Svalbard). Mar Biol Res 7:13-26

Reynolds PD (2006) Scaphopoda: The tusk shells. In: Sturm CF, Pearse TA, Valdes A (eds.) The Mollusks: A Guide to Their Study, Collection, and Preservation, pp. 229-237, Universal Publishers:Boca Raton.

Robinson RS, Keinast M, Albuquerque AL, Altabet M, Contreras S, De Pol Holz R, Dubois N, Francois R, Galbraith E, Hsu T-C, Ivanochko T, Jaccard S, Kao S-J, Keifer T, Kienast S, Lehmann M, Martinez P, McCarthy M, Möbius J, Pedersen T, Quan TM, Ryabenko E, Schmittner A, Schneider R, Schneider-Mor A, Shigemitsu M, Sinclair D, Somes C, Studer A, Thunell R, Yang J-Y (2012) A review of nitrogen isotopic alteration in marine sediments. Paleoceanography 27:PA4203

Rontani J-F, Charrière B, Sempéré R, Doxaran D, Vaultier F, Vonk JE, Volkman JK (2014) Degradation of sterols and terrigenous organic matter in waters of the Mackenzie Shelf, Canadian Arctic. Org Geochem 75(0):61-73

Rosenzweig ML (1971) Paradox of enrichment - destabilization of exploitation ecosystems in ecological time. Science 171:385–387

Roy V, Iken KI, Gosselin M, Tremblay J-É, Bélanger S, Archambault P (in review) Benthic food-web responses to marine biological productivity and depth across the Canadian Arctic. Deep-Sea Res Pt I

Sakshaug E (2004) Primary and secondard production in the Arctic seas. In: Stein R, Macdonald RW (eds.) The organic carbon cycle in the Arctic Ocean. Springer:Heidelberg, pp. 57-81

Saupe SM, Schell DM, Griffiths WB (1989) Carbon-isotope ratio gradients in western Arctic zooplankton. Mar Biol 103(4):427-432

Schell DM (1983) Carbon-13 and carbon-14 abundances in Alaskan aquatic organisms: delayed production from peat in Arctic food webs. Science 219(4588):1068-1071

Schell DM, Ziemann PJ, Parrish DM, Dunton KH, Brown EJ (1984) Foodweb and nutrient dynamics in nearshore Alaska Beaufort Sea waters. US Dep. Commerce, NOAA, OCSEAP Final Rep. 25, pp. 327–499.

Schell DM, Barnett BA, Vinette KA (1998) Carbon and nitrogen isotope ratios in zooplankton of the Bering, Chukchi and Beaufort seas. Mar Ecol Progr Ser 162:11-23

Schlitzer R (2011) “Ocean data view version 4.5.3” Alfred Wegener Institute for Polar and Marine Research, Bremerhaven, Germany

Shimada K, Itoh M, Nishino S, McLaughlin F, Carmack E, Proshutinsky A (2005) Halocline structure in the Canada Basin of the Arctic Ocean. Geophys Res Lett 32:L03605

Solomon CT, Cole JJ, Doucett RR, Pace ML, Preston ND, Smith LE, Weidel BC (2009) The influence of environmental water on the hydrogen stable isotope ratio in aquatic consumers. Oecologia 161(2):313-324

Søreide JE, Hop H, Carroll ML, Falk-Petersen S, Hegseth EN (2006) Seasonal food web structures and sympagic–pelagic coupling in the European Arctic revealed by stable isotopes and a two-source food web model. Prog Oceanogr 71(1):59-87

Soto DX, Wassenaar LI, Hobson KA (2013) Stable hydrogen and oxygen isotopes in aquatic food webs are tracers of diet and provenance. Funct Ecol 27:535-542

Sun M-Y, Carroll ML, Ambrose WG Jr, Clough LM, Zou L, Lopez GR (2007) Rapid consumption of phytoplankton and ice algae by Arctic soft-sediment benthic communities: evidence using natural and ^{13}C-labeled food materials. J Mar Res 65(4):561-588

Tank SE, Manizza M, Holmes RM, McClelland JW, Peterson BJ (2012) The processing and impact of dissolved riverine nitrogen in the Arctic Ocean. Estuar Coast 35:401-415

Telang SA, Pocklington R, Naidu AS, Romankevich EA, Gitelson II, Gladyshev MI (1991) Carbon and mineral transport in major North American, Russian Arctic, and Siberian rivers: the St. Lawrence, the Mackenzie, the Yukon, the Arctic Alaskan rivers, the Arctic Basin rivers in the Soviet Union, and the Yenisei. In: Degens ET, Kempe S, Richey JE (eds.) Biogeochemistry of major world rivers. Wiley: Chichester, pp 75-104

Tenore KR (1983) What controls the availability to animals of detritus derived from vascular plants: organic nitrogen enrichment or caloric availability? Mar Ecol Prog Ser 10:307-309

Terazaki M (1998) Life history, distribution, seasonal variability and feeding of the pelagic chaetognath *Sagitta elegans* in the Subarctic Pacific: a review. Plankton Biol Ecol 45(1):1-17

Thorp JH, Delong MD (2002) Dominance of autochthonous autotrophic carbon in food webs of heterotrophic rivers. Oikos 96(3):543-550

Thorton SF, McManus J (1994) Application of organic carbon and nitrogen stable isotope and C/N ratios as source indicators of organic matter provenance in estuarine systems: evidence from the Tay Estuary, Scotland. Estuar Coast Shelf Sci 38:219-233

Tremblay J-É, Michel C, Hobson KA, Gosselin M (2006) Bloom dynamics in early opening waters of the Arctic Ocean. Limnol Oceanogr 51(2):900-912

Tremblay J-É, Bélanger S, Barber DG, Asplin M, Martin J, Darnis G, Fortier L, Gratton Y, Link H, Archambault P, Sallon A, Michel C, Williams WJ, Philippe B, Gosselin M (2011) Climate forcing multiplies biological productivity in the coastal Arctic Ocean. Geophys Res Lett 38:L18604

Trenberth KE, Jones PD, Ambenje P, Bojariu R, Easterling D, Klein Tank A, Parker D, Rahimzadeh F, Renwick JA, Rusticucci M, Soden B, Zhai P (2007) Observations: surface and atmospheric climate change. In: Solomon S, Qin D, Manning M, Chen Z, Marquis M, Averyt KB, Tignor M, Miller HI (eds.) Climate Change 2007: The Physical science basis. Contribution of working group I to the fourth assessment report of the intergovernmental panel on climate change. Cambridge University Press: Cambridge, UK and New York, NY

Vallières C, Retamal L, Ramlal P, Osburn CL, Vincent WF (2008) Bacterial production and microbial food web structure in a large Arctic river and the coastal Arctic Ocean. J Mar Syst 74(3-4):756-773

Vander Zanden MJ, Rasmussen JB (1999) Primary consumer δ^{13}C and δ^{15}N and the trophic postion of aquatic consumers. Ecology 80(4):1395-1404

Vander Zanden MJ, Rasmussen JB (2001) Variation in δ^{15}N and δ^{13}C trophic fractionation: implications for aquatic food web studies. Limnol Oceanogr 46(8):2061-2066

Walsh JE (2008) Climate of the Arctic marine environment. Ecol Appl 18(2):S3-S22

Wassmann P (1998) Retention versus export food chains: processes controlling sinking loss from marine pelagic systems. Hydrobiologia 363:29-57

Wassmann P, Duarte CM, Agustí S, Sejr MK (2011) Footprints of climate change in the Arctic marine ecosystem. Global Change Biol 17(2):1235-1249

Williams WJ, Carmack EC, Shimada K, Melling H, Aagaard K, Macdonald RW, Ingram RG (2006) Joint effects of wind and ice motion in forcing upwelling in Mackenzie Trough, Beaufort Sea. Cont Shelf Res 26(19):2352-2366

Williams WJ, Carmack EC (2008) Combined effect of wind-forcing and isobath divergence on upwelling at Cape Bathurst, Beaufort Sea. J Mar Res 66(5):645-663

Witte U, Aberle N, Sand M, Wenzhöfer F (2003) Rapid response of a deep-sea benthic community to POM enrichment: an *in situ* experimental study. Mar Ecol Prog Ser 251:27-36

Wooller MJ, Zazula GD, Edwards M, Froese DG, Boone RD, Parker C, Bennett B (2007) Stable carbon isotope compositions of Eastern Beringian grasses and sedges: investigating their potential as paleoenvironmental indicators. Arct Antarct Alp Res 39(2):318-331

Yang C, Wilkinson GM, Cole JJ, Macko SA, Pace ML (2014) Assigning hydrogen, carbon, and nitrogen isotope values for phytoplankton and terrestrial detritus in aquatic food web studies. Inland Waters 4:233-242

Appendix A

Comparison of relative taxa distribution for biomass analysis

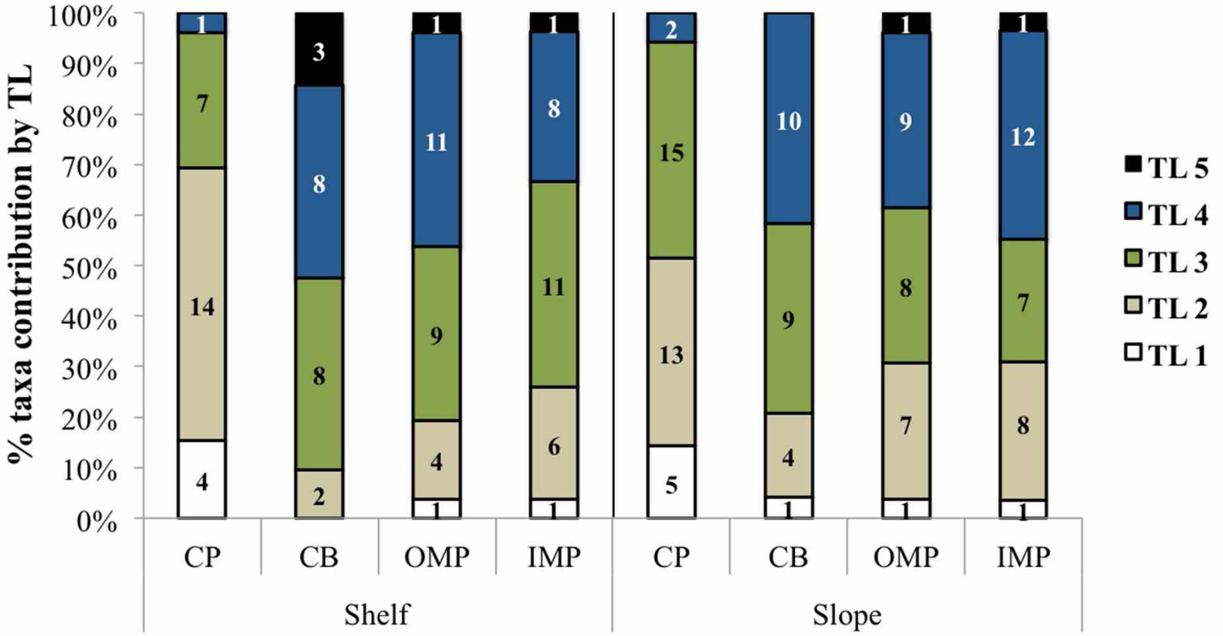

Figure A-1. Relative distribution of the number of taxa by trophic level for full taxon set. Trophic levels were determined based on primary consumer baseline. Histograms are grouped by region and depth group (shelf or slope), and labels indicate the number of taxa included in each bar section.

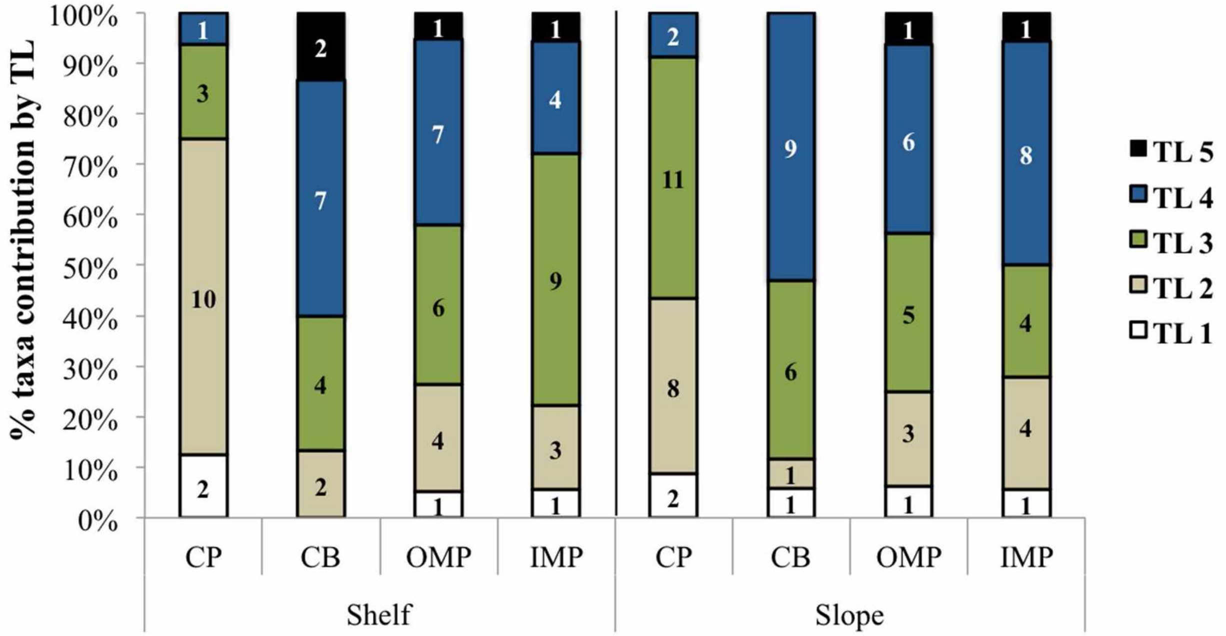

Figure A-2. Relative distribution of the number of taxa by trophic level including only the subset of taxa chosen for relative biomass comparison (see Fig. 10). Trophic levels were determined based on primary consumer baseline. Histograms are grouped by region and depth group (shelf or slope), and labels indicate the number of taxa included in each bar section.

Appendix B
2013 IACUC #134765-13 approval

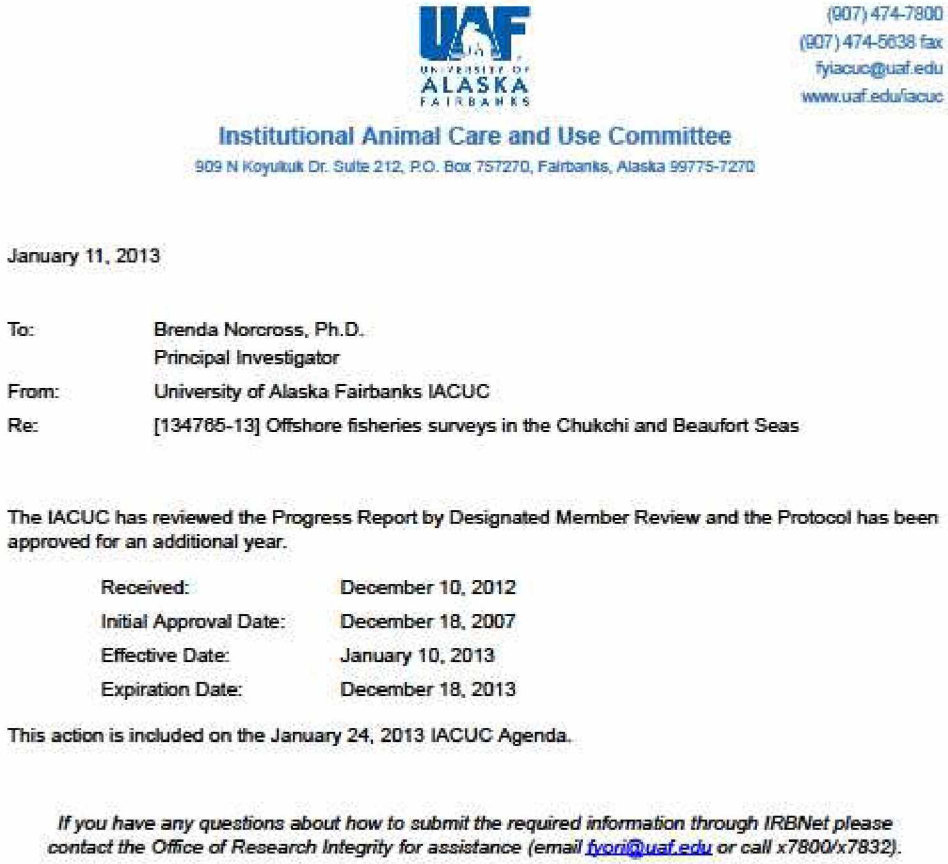

UNIVERSITY OF ALASKA FAIRBANKS

(907) 474-7800
(907) 474-5638 fax
fyiacuc@uaf.edu
www.uaf.edu/iacuc

Institutional Animal Care and Use Committee
909 N Koyukuk Dr. Suite 212, P.O. Box 757270, Fairbanks, Alaska 99775-7270

January 11, 2013

To:	Brenda Norcross, Ph.D. Principal Investigator
From:	University of Alaska Fairbanks IACUC
Re:	[134765-13] Offshore fisheries surveys in the Chukchi and Beaufort Seas

The IACUC has reviewed the Progress Report by Designated Member Review and the Protocol has been approved for an additional year.

Received:	December 10, 2012
Initial Approval Date:	December 18, 2007
Effective Date:	January 10, 2013
Expiration Date:	December 18, 2013

This action is included on the January 24, 2013 IACUC Agenda.

If you have any questions about how to submit the required information through IRBNet please contact the Office of Research Integrity for assistance (email fyori@uaf.edu or call x7800/x7832).

Appendix C
2014 IACUC #134765-14 Approval

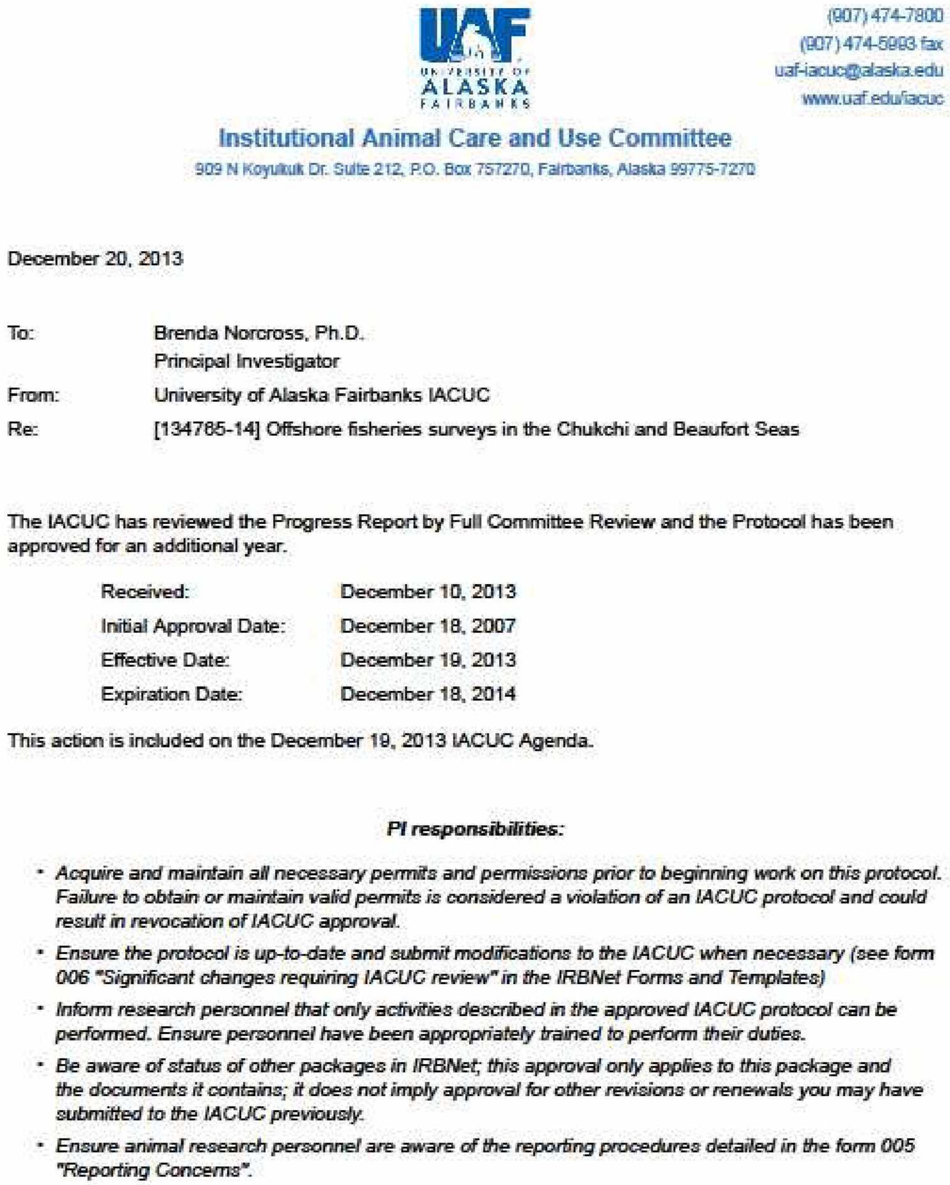

UNIVERSITY OF
ALASKA
FAIRBANKS

(907) 474-7800
(907) 474-5993 fax
uaf-iacuc@alaska.edu
www.uaf.edu/iacuc

Institutional Animal Care and Use Committee
909 N Koyukuk Dr. Suite 212, P.O. Box 757270, Fairbanks, Alaska 99775-7270

December 20, 2013

To: Brenda Norcross, Ph.D.
Principal Investigator
From: University of Alaska Fairbanks IACUC
Re: [134765-14] Offshore fisheries surveys in the Chukchi and Beaufort Seas

The IACUC has reviewed the Progress Report by Full Committee Review and the Protocol has been approved for an additional year.

Received: December 10, 2013
Initial Approval Date: December 18, 2007
Effective Date: December 19, 2013
Expiration Date: December 18, 2014

This action is included on the December 19, 2013 IACUC Agenda.

PI responsibilities:

- *Acquire and maintain all necessary permits and permissions prior to beginning work on this protocol. Failure to obtain or maintain valid permits is considered a violation of an IACUC protocol and could result in revocation of IACUC approval.*
- *Ensure the protocol is up-to-date and submit modifications to the IACUC when necessary (see form 006 "Significant changes requiring IACUC review" in the IRBNet Forms and Templates)*
- *Inform research personnel that only activities described in the approved IACUC protocol can be performed. Ensure personnel have been appropriately trained to perform their duties.*
- *Be aware of status of other packages in IRBNet; this approval only applies to this package and the documents it contains; it does not imply approval for other revisions or renewals you may have submitted to the IACUC previously.*
- *Ensure animal research personnel are aware of the reporting procedures detailed in the form 005 "Reporting Concerns".*